Reviews in Mineralogy & Geochemistry
Vol. 78 pp. 745-777, 2014
Copyright © Mineralogical Society of America

High-pressure Apparatus Integrated with Synchrotron Radiation

Guoyin Shen

HPCAT, Geophysical Laboratory
Carnegie Institution of Washington
Argonne, Illinois 60439, U.S.A.

gshen@ciw.edu

Yanbin Wang

Center of Advanced Radiation Sources
University of Chicago
Chicago, Illinois 60637, U.S.A.

wang@cars.uchicago.edu

INTRODUCTION

Synchrotron sources provide X-radiation with high energy and high brilliance that are well suited for high-pressure (HP) research. Powerful micron-sized sampling probes of high energy radiation have been widely used to interact with minute samples through the walls of pressure vessels, to investigate material properties *in situ* under HP. Since the late 1970s, HP synchrotron research has become a fast growing field. Of mineralogical interests are the abilities for studying structure, elasticity, phase stability/transition, and transport properties of minerals and melts at pressure-temperature conditions corresponding to the deep Earth.

The most commonly used HP apparatus are the diamond anvil cell (DAC), the large volume press (LVP), and the shock wave devices. The DAC is capable of generating pressures beyond 4 megabar (1 megabar = 100 GPa) but is limited to small samples, typically less than 10 microns in linear dimensions at the highest pressures. The pressure-temperature (*P-T*) range accessible in the DAC exceeds conditions corresponding the center of the Earth. The LVP is capable of modest pressures (currently less than 100 GPa), but the large sample volume permits a wider variety of bulk physical properties to be measured. The *P-T* range accessible in the LVP corresponds to those in the Earth's lower mantle. In shock wave experiments, the sample is subjected to high pressures and temperatures by dynamic processes. Multi-megabar to terapascal (TPa) pressures may be generated but for short durations from nano- to femto-seconds (10^{-9}-10^{-15} s).

In this chapter, we begin with synchrotron techniques that are important for HP research, followed by a review of high pressure apparatus and their integration with synchrotron X-ray techniques. We refer readers to the following review articles related to HP synchrotron techniques (Chen et al. 2005; Duffy 2005; Hemley et al. 2005; Wang et al. 2002b).

1529-6466/14/0078-0018$05.00 http://dx.doi.org/10.2138/rmg.2014.78.18

SYNCHROTRON TECHNIQUES APPLICABLE TO HIGH-PRESSURE RESEARCH

Synchrotron radiation

Synchrotron radiation is produced by free relativistic electrons moving along curved trajectories in a magnetic field. Research using synchrotron radiation began at storage rings designed and operated for high energy physics. At these so-called first generation synchrotron sources, the use of synchrotron radiation was of secondary importance and X-ray stations were operated parasitically. Starting in the mid-1970s, second-generation synchrotron facilities were designed and built to serve as dedicated X-radiation sources (e.g., Hartman 1982). In the late-1980s, insertion device based sources (the third generation) were built and began their operation in the early 1990s (Mills 2002). Great efforts have been made to take advantages of the unique characteristics of synchrotron radiation for HP research, including: 1) high intensity in a broad energy spectral range, 2) high brilliance (small angular divergence), 3) tunable energy with the use of monochromators, 4) pulsed time structure, 5) coherence, and 6) high polarization of the radiation. A number of HP beam-lines have been or are being built in synchrotron facilities in the US [the Advanced Light Source (ALS), Stanford Synchrotron Radiation Lightsource (SSRL), National Synchrotron Light Source (NSLS), Cornell High Energy Synchrotron Source (CHESS), the Advanced Photon Source (APS)], in Europe [European Synchrotron Research Facility (ESRF), Soleil, Diamond, Petra-III, MAX-IV], and in the Asia-Pacific [Photon Factory, Spring-8, Beijing Synchrotron Research Facility (BSRF), Shanghai Synchrotron Research Facility (SSRF), Taiwan Photon Source (TPS), Puhong Light Source (PLS), and the Australia Synchrotron (AS)]. The webpage (http://www.lightsources.org) has a comprehensive list of synchrotron sites in the world with relevant links for more information.

Synchrotron radiation provides the necessary penetration power to go through the walls of pressure vessels. Figure 1 shows transmission of commonly-used wall materials as a function of X-ray energy. The high brilliance of synchrotron radiation has made it possible for the developments of various HP synchrotron techniques. Continuously tunable wavelength opens up new capabilities, in particular in HP X-ray spectroscopy and HP inelastic X-ray scattering (Mao et al. 1997; Fiquet et al. 2001; Rueff 2010). The pulsed timing structure, together with the high brilliance, allows the study of time dependent phenomena such as phase transition

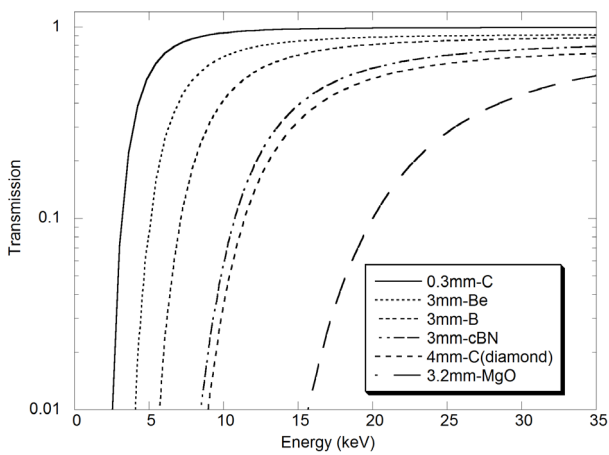

Figure 1. X-ray transmission curves of commonly used materials in high pressure devices. Curves from left to right correspond to materials in the legend from top to bottom.

kinetics, chemical reaction processes, transport processes, and meta-stable phases at high pressures and high/low temperatures (Jensen et al. 2012; Luo et al. 2012). The polarization of synchrotron radiation has been extensively utilized for investigations of magnetic systems at high pressure (Haskel et al. 2011; Souza-Neto et al. 2012). While coherence has been used for mapping structure and strain in nanometer-scale grains (Pfeifer et al. 2006), HP applications are still in its infancy (Le Bolloch et al. 2009; Yang et al. 2013). It should be noted that recently constructed synchrotron facilities have achieved a high degree of orbit stability, providing highly stable X-ray beams in terms of intensity and position, critical for HP experiments.

Worldwide there are growing activities in the development of free-electron lasers (FELs) (Galayda et al. 2010), such as the Linac Coherent Light Source (LCLS) in the US, the SPring-8 Compact SACE Source (SCSS) in Japan, and the European X-ray Free-Electron Laser (XFEL). These so-called fourth generation sources offer spatially highly coherent, ultra-short (~100 fs) pulses with peak brilliance of ~10^{28}-10^{33} photons/s/mm^2/mrad^2/0.1%BW. Figure 2 shows the FEL brilliance compared with those of earlier synchrotrons. In the storage rings of synchrotron radiation facilities, the radiated intensity is linearly proportional to the number of electrons in the beam, because of the lack of multi-particle coherence. In FELs, however, the electron beam is bunched together on the scale of the radiation wavelength, resulting in a high degree of multi-particle coherence, significantly enhancing the emission brilliance. The spatially coherent high intensity, short pulsed X-ray beams open up many new areas, including time-resolved studies of dynamics on sub-ps time scales, structural studies by imaging of nano-periodic systems, and probing warm dense matter—a state too dense to be described by weakly coupled plasma physics and too hot to be described by condensed matter physics. Warm dense matter is expected in the cores of some large planets. Important to HP research, significant effort has been made to produce harder X-rays with energies at 16 keV or higher in the FEL facilities. For example, an experimental station at LCLS for Matters in Extreme

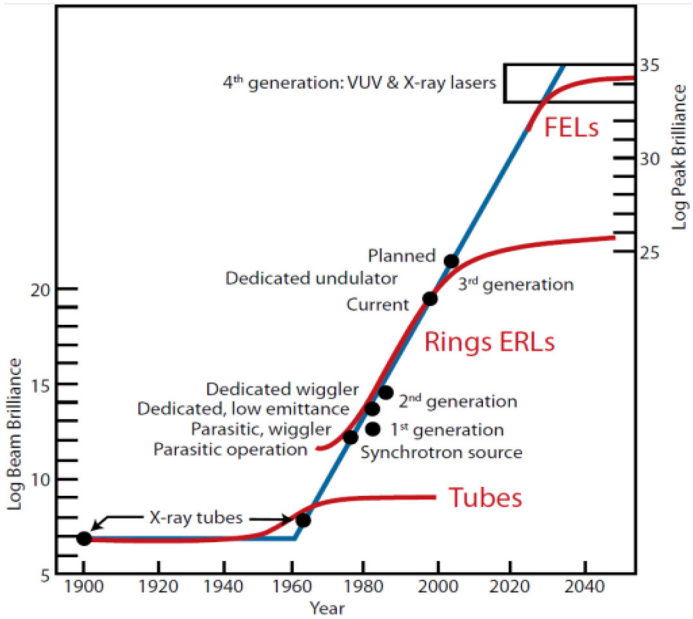

Figure 2. X-ray brilliance with orders of magnitude increase with time. Tubes represent X-tubes generally used in laboratory, "Rings": storage rings of synchrotron facilities, "ERLs": energy recovery LINACS, FELs: free electron lasers (Courtesy of M. Rivers).

Condition has recently become operational since 2012 for warm condensed physics, high pressure studies, shock physics, and high energy dense physics.

High-pressure synchrotron techniques

High-pressure research has become an important application area for synchrotron sources. Many previous technical limitations in capability, precision, and accuracy have been removed through optimization of source radiation, optics, sample environment, experimental configuration, motion control, automation software, and detectors and analyzers. Among the wide array of HP X-ray techniques, structure determination using X-ray diffraction (XRD) remains the dominant one, while significant progress has been made in integrating other X-ray techniques for HP research, such as X-ray radiography and tomography (Shen et al. 2002; Wang et al. 2005a; Wang et al. 2012), X-ray spectroscopy (absorption, emission) (Mao et al. 1997; Mayanovic et al. 2007b), inelastic X-ray scattering (IXS) (Rueff 2010), and nuclear resonant scattering (Cainrs et al. 1976; Lübbers et al. 2000; Sturhahn 2004). New HP synchrotron techniques are emerging rapidly, for example in HP nano-imaging techniques (full field, scanning, and coherent diffraction) (Le Bolloch et al. 2009; Wang et al. 2012) and time resolved HP X-ray techniques (Goncharov 2010; Yoo et al. 2011; Luo et al. 2012). A few firsts of HP experiments integrated with synchrotron techniques are listed in Table 1.

Table 1. Firsts of high-pressure experiments integrated with synchrotron techniques.

Technique	Abbr.	Reference
HP X-ray diffraction	XRD	(Buras et al. 1976)
HP X-ray absorption spectroscopy	XAS	(Ingalls et al. 1978)
HP X-ray emission spectroscopy	XES	(Rueff et al. 1999)
HP inelastic X-ray scattering (eV)	IXS	(Schell et al. 1995)
HP inelastic X-ray scattering (meV)	IXS	(Fiquet et al. 2001)
HP nuclear resonant inelastic X-ray scattering	NRIXS	(Lübbers et al. 2000)
HP nuclear forward X-ray scattering	NFXS	(Nasu 1996)
HP X-ray fluorescence spectroscopy	XFS	(Schmidt and Rickers 2003)
HP X-ray computed micro-tomography	CMT	(Wang et al. 2005a)

HP X-ray diffraction. X-ray diffraction (XRD) has long been the dominant application of synchrotron radiation for HP research. Samples in various forms (single crystal, polycrystalline, nano-crystals, amorphous/liquid) have been studied in HP XRD for structure and/or radial distribution functions, phase transitions (including melting), *P-V-T* equations of state, elasticity, and lattice strain.

Angular dispersive XRD (ADXRD) using monochromatic radiation and two dimensional (2D) detectors has been the primary technique in DAC experiments. Resolution in ADXRD is typically at $\Delta d/d \sim 3\times10^{-3}$ (e.g., Shen et al. 2008). The resolution in d-spacing can be improved by reducing incident beam divergence, lowering X-ray energy, and improving angular resolution in detecting systems by, for example, increasing sample-detector distance, reducing slit size or effective pixel size, or using an analyzer. High resolution is achieved at the cost of throughput; proper approaches need to be planned in advance. Intensity information in ADXRD is often used for structure refinement via Rietveld method (Rietveld 1966). However, background subtraction for removing intensity contributions from the surrounding materials (anvils, gaskets) is not trivial and precautions need to be taken when using Rietveld

refinement and interpreting the results from those analyses. Recently, there has been a growing effort in measuring pair distribution functions (PDF) of amorphous/liquid materials at HP where background subtraction has been critically tested (Eggert et al. 2002; Shen et al. 2003; Chapman et al. 2010; Soignard et al. 2010). The developed methods for background subtraction can be also applied to Rietveld refinement on crystalline samples. In HP ADXRD, typical X-ray energy is around 15-45 keV in DAC experiments, based on factors such as the coverage in reciprocal space, accessing angular range of the high pressure device, penetrating power, and detector efficiency. Nevertheless, a wide range from 10 keV to over 100 keV has been used for various applications. The energy tunability of synchrotron sources should allow for HP anomalous diffraction studies for solving the phase problem, partial structure factor, and element specific crystallography. To our knowledge, however, there is no report of HP anomalous XRD yet.

The primary technique in LVP experiments has been energy-dispersive XRD (EDXRD). This is mainly due to two factors: 1) in most multi-anvil devices X-ray access is limited because of the opaque anvil materials used and 2) the sample is often contained by solid pressure media which may generate overpowering scattering background if the incident beam and scattering signals are not properly collimated. EDXRD is ideal for phase identification and equation of state studies in the LVP. Data collection is fast (from seconds to minutes), and clean diffraction signals can be obtained, despite pressure media surrounding the sample. Metal capsules are often used to control the sample environment (oxygen fugacity, water content, etc). However, EDXRD provides limited sampling of crystallites in the sample because of the fixed 2θ angle, and is not suitable for probing samples near melting or with rapid crystal growth, in which case ADXRD with an area detector is desired and light scattering materials are used as "windows" (e.g., Kubo et al. 2008).

Another limitation is that EDXRD does not provide reliable intensity measurements, making it difficult to obtain crystal structure information such as bonding characteristics and atomic positions. Various efforts have been made to extract quantitative crystallographic information from EDXRD data, with limited success (e.g., Ballirano and Caminiti 2001; Skelton et al. 1982; Yamanaka and Ogata 1991). Wang et al. (2004) developed a technique which employs both ADXRD and EDXRD concepts. By scanning an energy-calibrated multichannel solid state detector (SSD), a large number of EDXRD patterns are obtained at pre-determined angular step-size. The entire dataset can be re-arranged as ADXRD patterns by plotting intensities of each channel (corresponding to a given photon energy or wavelength). Subsets of the data covering narrow energy bands may be binned to give ADXRD patterns at a single wavelength with improved counting statistics; these may be combined in a multi-pattern Rietveld analysis to efficiently utilize the entire data set: while high photon-energy data provide coverage at the low *d*-spacing range, low photon-energy data cover the high d-spacing range. An example is shown in Figure 3, for the identification on non-cubic structure of $CaSiO_3$ perovskite (Uchida et al. 2009).

When a sample is subjected to a boundary condition with a differential stress component, diffraction in a radial geometry may be applied with the loading axis perpendicular to the primary X-ray direction, a DAC diffraction technique called radial X-ray diffraction (R-XRD). In specially designed multianvil devices such as the deformation DIA (Wang et al. 2000, 2003) or rotational Drickamer apparatus (Yamazaki and Karato 2001), R-XRD is used to measure stresses in a sample under controlled differential stress field during deformation. Strains can be easily measured using radiography, hence permitting measurements of stress-strain curves of bulk samples at high P and T (e.g., Hilairet et al. 2007; Nishiyama et al. 2007). HP R-XRD provides useful information on sample stress, strain, deformation, and slip mechanism (Wenk et al. 2000, 2005; Merkel et al. 2006; Hilairet et al. 2012), by measuring diffraction as a function of the angle between the loading axis and the vector of diffraction plane. The

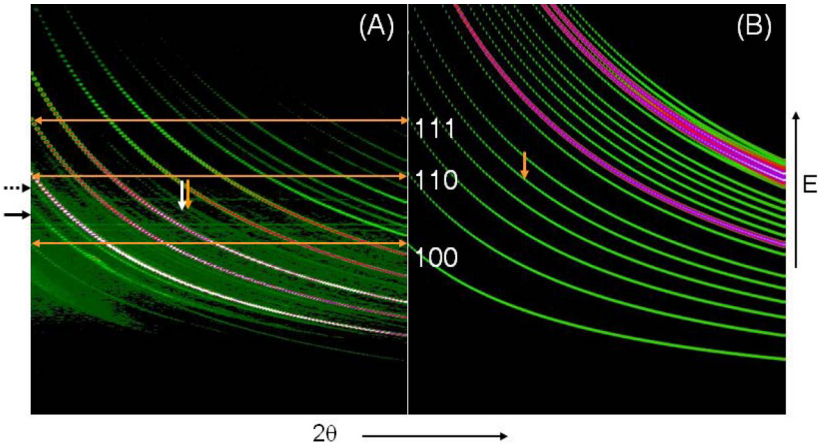

Figure 3. An example of multi-angle EDXD diffraction for $CaSiO_3$ perovskite. Horizontal axes are two-theta angle from 3° to 13°, at s step size of 0.05°, vertical axes are X-ray energy from ~0 to 150 keV. (A) Experimental data collected at 13 GPa and 1200 K. Intensities are plotted in logarithmic scale. (B) Simulated $CaSiO_3$ perovskite pattern assuming cubic (P*m3m*) symmetry. Experimental data in (A) show clear superlattice reflections (indicated by horizontal arrows), indicating non-cubic symmetry. The vertical arrows in (A) and (B) indicate the cubic (200) diffraction line. Figure modified after Uchida et al. (2009).

dependence of *d*-spacings as a function of the angle provides information on strains under deviatoric stress conditions. The relative intensity at different angles reveals the preferred orientation of a polycrystalline sample. The inverse pole figure from such data can be used to determine sample deformation and slip mechanism (e.g., Miyagi et al. 2010).

Compared to the most frequently used HP powder XRD techniques at synchrotron HP beamlines, HP single crystal XRD is relatively under-utilized, but it is a fast developing field (Lavina et al. 2014, this volume). In single crystal XRD, orientations and intensities of diffracted beams are measured. The high flux and small beam at synchrotron HP beamlines allow for studies with 1-10 micron crystal size efficiently. Detailed crystallographic information, such as structure model (atomic position, occupancies, thermal displacement parameters) and electron density distribution can be obtained (Fig. 4). With single crystal data, space groups and Miller indices can be unambiguously determined. Because the diffraction is measured at different orientations, the single crystal XRD technique has also advantages in dealing with materials of low crystallographic symmetries. HP single crystal XRD was first applied to the EDXRD method (Mao et al. 1988; Loubeyre et al. 1996). Recently, synchrotron monochromatic beam has been widely used in HP single crystal XRD by rotating samples coupled with either a point detector (Friedrich et al. 2007) or an area detector (Lavina et al. 2010; Zhang et al. 2013). Many HP beamlines in the world have established routine procedures for conducting HP single crystal XRD experiments.

When there are constraints in rotating the sample, HP single crystal XRD experiments may be conducted by scanning monochromatic energies with an area detector (Ice et al. 2005). The use of polychromatic beam (the Laue approach) is a useful alternative. The HP Laue approach does not require rotating of the sample and could provide information on deformation, mosaicity, and strains (Ice and Pang 2009) through fast measurements (less than a second).

HP XRD has been widely used to determine structure factors of amorphous/liquid materials at HP (Tsuji et al. 1989; Shen et al. 2003; Wilding et al. 2006). Interesting phenomena have been observed, including coordination number change, polyamorphysm (Katayama

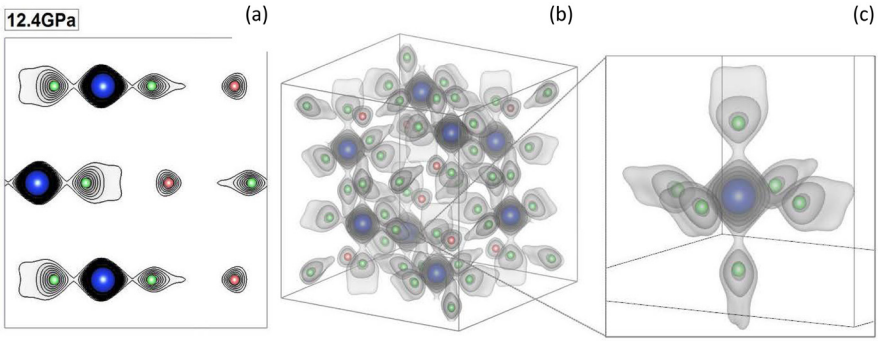

Figure 4. Electron density distributions in silicon at high pressures. (a) and (b) are the electron density data at 12.4 GPa where the two active groups are clearly observed; (a) a slide image along the [110] plane. The host lattice of the α-phase is represented by the symbols in blue. The void group is shown in red, while the vicinity group in green. The local distribution of the vicinity group has the point-group symmetry of S_4 as shown in (c). Modified from Shen et al. (2012).

et al. 2000; Deb et al. 2001), and long-range topological order (Zeng et al. 2011). In DAC experiments, the ADXRD method is often utilized with high energy monochromatic beam in order to have a large Q coverage (Chapman et al. 2010; Mei et al. 2010; Soignard et al. 2010). The EDXRD method with polychromatic radiation is often used in LVP experiments. EDXRD data are collected at multiple 2θ angles, to increase coverage in the reciprocal space for accurate determination of the radial distribution function (e.g., Tsuji et al. 1989). The synchrotron incident beam spectrum is simulated using a Monte Carlo approach and Compton scattering effects are typically dealt with based on theoretical predictions (Funakoshi 1995). The advantage of this method is the excellent collimation, through which background scattering from surrounding materials can be almost completely eliminated (Yamada et al. 2011; Sakamaki et al. 2012). This is a particularly useful technique for liquids with low scattering power (e.g., oxides and silicates). With the use of a Soller slit system, diffraction from surrounding materials can be effectively minimized and ADXRD has been successfully applied for studying liquid structures at HP and HT with LVPs such as the Paris-Edinburgh (PE) presses (Mezouar et al. 2002).

HP X-ray spectroscopy. The last decade saw rapid development for HP X-ray spectroscopy (XRS). Many new HP XRS capabilities have been enabled and established at several HP beamlines around the globe. With emerging new synchrotron sources and upgrades of many existing third generation sources, together with developments and optimization efforts of HP devices designed for HP XRS, we are entering a harvesting period for HP research using XRS.

X-ray absorption spectroscopy (XAS) is a classic technique that measures energy dependence of X-ray absorption coefficient for a core-level electron of an element of interest. Near edge X-ray absorption spectroscopy (XANES) provides information on valence state, orbital-occupancy, hybridization, charge transfer, and electronic ordering. Extended X-ray absorption fine structure (EXAFS) provides element specific local structural information. XAS is one of the first XRS technique applied for HP research (Ingalls et al. 1978). However, earlier applications of HP XAS were limited to a small energy range due to anvil absorption and Laue diffraction from single crystal anvils. Recently, perforated and partially-perforated diamond anvils have been used to successfully reduce the amount of diamond scattering in the beam path. High quality HP XANES (Zeng et al. 2010) and HP XAFS (Mayanovic et al. 2007a) data have been collected for transition metals in DAC experiments with energies between 5 and15 keV. In studying absorption edges over 30 keV, XAS data from a DAC are

contaminated by diffraction from single-crystal diamond anvils. Using nano-diamond as anvil material, the contamination from single crystal diffraction can be avoided (Ishimatsu et al. 2012). Morard et al. (2007a) reported results on the Ba K-edges (>37 keV) in silicon clathrate (Ba_8Si_{46}), tracking the evolution of local structure around Ba with pressure. These authors also examined iodine K-edges in iodine-intercalated single-wall carbon nanotubes, to understand the local structure of iodine in this material at high *P* and *T*.

At ESRF, an energy dispersive XRS (EDXRS) technique has been developed (Pascarelli and Mathon 2010), in which a focused polychromatic beam (~5 μm) of extremely high flux passes a sample, and is collected by an energy dispersive detector capable of fast capturing the HP XAS signals at micro-second level (Boehler et al. 2009; Andrault et al. 2010). The fast measurement and small beam size in EDXRS allow for mapping XAS images by scanning the sample position (Aquilanti et al. 2009).

When the HP environment is coupled with circularly (or linearly) polarized X-ray radiation and magnetic fields, the related X-ray magnetic circular (or linear) dichroism (XMCD or XMLD) techniques can be used to yield information on spin-polarized electronic structure, magnetic ordering, and magnetization (Iota et al. 2007; Gorria et al. 2009; Haskel et al. 2011; Souza-Neto et al. 2012).

XAS in the LVP is currently limited to photon energies above ~10 keV due to the solid pressure media used in cell assemblies that attenuate the signal. The advantage of using an LVP for XAS, on the other hand, is uniform and stable heating over a large sample volume. Both the DIA and PE press have been used for XAS studies. Yoshiasa et al. (1999) studied *P* and *T* dependence of EXAFS Debye-Waller factors in diamond-type and white-tin-type Ge to 11 GPa and 700 K; Arima et al. (2007) collected EXAFS spectra for liquid AgI up to 1200 K, to investigate pressure-induced local structural change. Both studies were conducted in the DIA apparatus at Spring-8. Coppari et al. (2008) studied local structure of liquid Cu to 4 GPa and 1350 °C using XAS in the PE cell at ESRF.

While XAS provides information on valence electrons and unoccupied density of states, X-ray emission spectroscopy (Feás et al. 2009) characterizes core electrons and occupied density of states through processes of excitation of the core electron as well as its decay to fill the core-level vacancy. This process is characteristic of an atom with weak influence of nearest neighbor species. For example, side-bands of the K_β emission line for several 3d transition metals provide signatures of spin, valence, and bonding information. In HP XES experiments, emission X-rays are collected by a θ-2θ scan of the analyzer and the detector in a Rowland circle (~1-meter in diameter) (Rueff et al. 1999). The spherically-bent, sub-eV analyzers are about 100 mm in diameter. Because emission signals can be collected at any direction, multiple analyzers may be used to increase solid angle coverage in data collection and thus the signal level. Recently, a short-distance spectrometer of large solid angle coverage has been developed, with which data collection time in HP XES is reduced from hours to only several minutes (Pacold et al. 2012) (Fig. 5). XES has been widely used to study pressure induced spin transitions of earth materials (Rueff et al. 1999; Badro et al. 2003; Lin et al. 2004). The band width change as a function of pressure was probed by HP XES for a semiconducting material (Ge) (Struzhkin et al. 2006).

Resonant XES (RXES), or partial fluorescence yield (PFY), has also been successfully utilized in HP research. HP RXES may be viewed as a combination of XES and XAS. Instead of collecting transmitted X-rays as in XAS, emission spectra are measured at each step as the incident beam energy is changed or scanned across an absorption edge. This resonant method significantly enhances footprints of electron states, and has a remarkable sharpening effect in projected spectra (RXES or PFY) (Rueff 2010; Wang et al. 2010a). RXES spectra have allowed for resolving crystal-field splitting of Fe^{3+} in Fe_2O_3 at HP (Wang et al. 2010a) and intermediate spin state of Fe_3O_4 at 15-16 GPa (Ding et al. 2008).

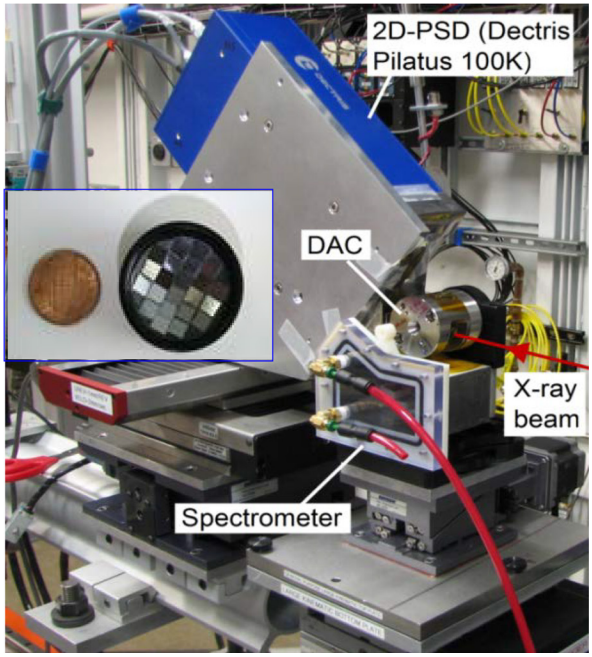

Figure 5. Setup of a short distance XES spectrometer (miniXES) at HPCAT, APS. The collection solid angle is ~50 msr (inset), about six times more than the traditional spherically-bent crystal analyzer.

HP X-ray fluorescence spectroscopy (HP XFS) permits determination of solubility of minerals in fluids at HP (Schmidt and Rickers 2003; Tanis et al. 2012). The method can be used for multi-element analytical probes and for studies of dissolution kinetics (Schmidt et al. 2007). In XFS experiments the fluorescence signals (e.g., K_α, K_β, or both) are collected by a solid-state energy dispersive detector. Currently, the detection limit for HP XFS is at a few ppm level for elements down to atomic number 22 (Ti) to a pressure of 10 GPa at high temperatures to at least 1273 K (Petitgirard et al. 2009). A confocal geometry has been developed for minimizing unwanted background signals (Wilke et al. 2010), further improving the efficiency and consequently detection limit.

HP Inelastic X-ray scattering. Inelastic X-ray scattering (IXS) has been successfully employed at the third generation synchrotron sources to study electronic and vibrational excitations in materials. HP research can now be conducted using non-resonant IXS, resonant IXS (RIXS), and nuclear resonant IXS (NRIXS). IXS may be performed with energy resolutions of 20 meV to 1 eV for electronic excitations and from sub-eV down to 0.5 meV for vibrational properties. Unlike chemical doping which introduces disorder and charge carriers, pressure provides a clean tuning mechanism that directly modifies electronic and phonon structures. Through HP IXS, fundamental properties of electron gas, strongly correlated systems such as superconducting materials, high-energy electronic excitations, and phonons in energy and momentum space can be obtained, providing critical data for code validation and tests of fundamental theories.

HP non-resonant IXS with ~1 eV energy resolution (often called X-ray Raman spectroscopy) is emerging as a powerful spectroscopic probe. HP soft X-ray spectra may be acquired with high energy X-rays which provide penetrating power through walls of a HP device. Combined with micro-focusing techniques, HP IXS can be applied to minute samples at HP (Shukla

et al. 2003; Lee et al. 2008; Mao et al. 2010). For example, K edges of light elements (Be, B, C, N, O, …) under HP conditions can be measured by HP IXS. Figure 6 shows the HP IXS data for graphite. Pressure-induced bonding change can be monitored through the carbon K edge. The narrow π* features at low energy are related to the 2π antibonding orbital, while the broad humps at high energy side corresponds to σ* in-plane bonds. Under pressure, partial suppressions of π bonding have been observed (Mao et al. 2003; Lin et al. 2011).

High energy resolution to meV level allows for studying lattice dynamics. Dynamical properties of materials under HP have been studied by using high energy resolution IXS (HERIXS, at ~1 meV energy resolution). Sound velocities of materials at HP to over 1 Mbar have been measured (Fiquet et al. 2001; Antonangeli et al. 2010, 2011) using this technique. With single crystal samples, complete phonon dispersions in the Brillouin zone may be mapped by HERIXS at HP (Farber et al. 2006). However, lattice dynamical data at HP are still limited, largely due to constraints by the strict requirements of sample quality, hydrostaticity, and, to some extent, beam time availability.

When the incident X-ray energy is chosen such that it coincides with one of the atomic X-ray absorption edges, resonance can greatly enhance the inelastic scattering cross section and create an excited immediate state. In resonant IXS (RIXS), the absence of a high energy core-hole in final state leads to intrinsically sharp spectra with energy and momentum. By tuning to different X-ray edges, RIXS provides element and orbital specific information. HP RIXS has been applied to various strongly correlated *d*-electron compounds (Shukla et al. 2003; Rueff 2010) and Kondo-like *f*-electron delocalization (Maddox 2006; Bradley et al. 2012).

In nuclear resonant IXS (NRIXS), incident X-rays of meV resolution is tuned near the exceedingly narrow nuclear resonant line (at neV level). By using time discrimination electron-

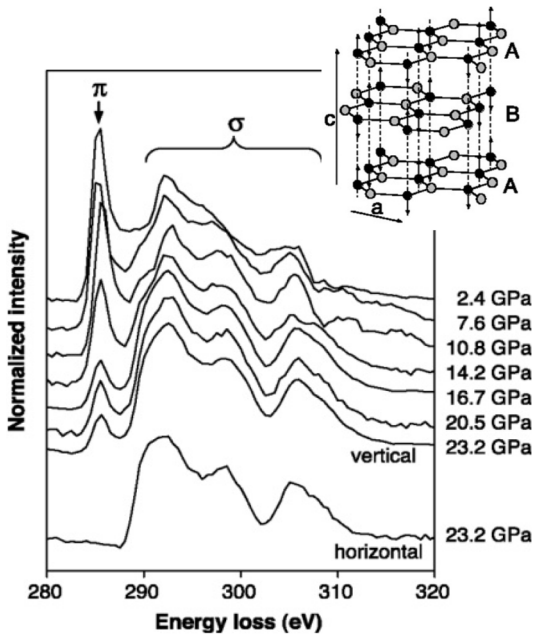

Figure 6. HP IXS spectra for graphite in two different experimental directions. The spectra in the vertical direction probe the inter-plane bonding, while those in the horizontal direction probe in-plane bonding. Insert: Graphite structure showing bridging carbon atoms (black spheres), which pair with an atom in an adjacent layer to form a σ-bond. Modified after Mao et al. (2003).

ics, the delayed signals caused by the narrow nuclear absorption provide NRIXS data (Sturhahn 2004). Of interest in mineral physics are measurements of phonon density of states and subsequent derivation of the Debye sound velocity (Wicks et al. 2010; Murphy et al. 2011b), which distinguishes compression and shear wave velocities as well as their temperature and pressure dependence. This technique also allows determination of anisotropy of sound velocities, and mode Grüneisen constants (Murphy et al. 2011a). HP NRIXS has been combined with laser heated diamond anvil cell to measure Debye sound velocities at HP and HT (Zhao et al. 2004; Lin et al. 2005b).

Nuclear forward scattering (NFS) using synchrotron radiation has been applied to studying Mössbauer effects at HP. Because of the high brilliance and highly focused beam, NFS is well suited for, and has been extensively used in, HP research. The NFS hyperfine signals are very sensitive to internal magnetic fields, electric field gradients, and isomer shifts, and are widely used in years to study magnetic collapse (Li et al. 2004b; Lin et al. 2005a), site occupancy (Catalli et al. 2011; Lin et al. 2012), and valence and spin state (Jackson et al. 2005; Speziale et al. 2005; Shim et al. 2009; Chen et al. 2012). Readers may refer to the reference by Sturhahn (2004) for a comprehensive description of the principle and experimental methods of the NFS technique. Compared to other nuclear resonant techniques, NFS measures the transmission signals which are relatively strong and may be collected in a fast manner. For example, fast NFS experiments have been performed to determine HP melting temperatures of iron by measuring the Lamb-Mössbauer factor which describes the probability of recoilless absorption (Jackson et al. 2013).

HP X-ray imaging. From the beginning of HP synchrotron experiments, HP X-ray imaging techniques have been used for locating HP sample position and defining sample shape. Now, a variety of HP X-ray imaging techniques have been developed for different imaging purposes, such as HP radiography, HP tomography, using the full-field imaging method or the position scanning method. Recently, HP coherent X-ray diffraction is being developed for nano-size materials (Le Bolloch et al. 2009; Yang et al. 2013).

HP radiography provides density contrast information through which the sample configuration inside the pressure device may be visible. Often times, because of the small beam in HP synchrotron experiments, radiography images are obtained by scanning sample positions. The position scanning radiography is essential in almost all HP synchrotron experiments and provides information on sample allocation, sample configuration, anvil deformation (Hemley et al. 1997), etc. By selecting proper monochromatic beams, absorption intensity contrast may be used for density determination for amorphous and liquid materials (Katayama et al. 1996; Shen et al. 2002; Hong et al. 2007).

It should be noted that the position scanning imaging method can be applied in any X-ray measurements. For example, by fast XAS measurements, images in chemical compositions and valence states may be obtained (Aquilanti et al. 2009). With increased brilliance and detection efficiency, many other measurements, such as XRD, XES, NFS (Mössbauer), may be used for mapping samples, providing images based on information of structure, valence state, spin, site occupancy etc. HP scanning imaging has great potential for detailed information not only from a single spot but from the entire sample. The image resolution in the position scanning method is limited by the beam size. Currently, all top DAC beamlines in the world have a typical beamsize of ~3-5 μm. Further reducing beam size to sub-μm is an important step in improving resolution in the scanning imaging techniques.

HP radiography can also be obtained by the full-field method, in which the incident beam is large relative to the sample size. Intensities of the transmitted X-rays are monitored by a phosphor screen which converts X-ray contrast into visible light, and recorded by a camera. The full-field radiography is fast, allowing for efficient recording the dynamic processes

in HP experiments. For example, a probing sphere can be *in situ* monitored for viscosity measurements of liquids at HP (Kanzaki et al. 1987; Rutter et al. 2002; Kono et al. 2013). High pressure melting processes can be recorded and the onset of melting may be defined (Dewaele et al. 2010). Phase contrast imaging measurements for bulk scale shock dynamic experiments have been demonstrated recently (Jensen et al. 2012; Luo et al. 2012). The full-field method may be also of high resolution (at sub-μm level), permitting precise determinations of sample dimensions. For example, full-field radiography is often used in HP ultrasonic measurements for sample dimensions. X-ray focusing optics (e.g., zone-plate) may be used as an "objective" similar to an optical microscope. With this, the resolution in full-field imaging can be increased significantly at the cost of the field-of-view. Such an X-ray microscope has a typical resolution of ~20-30 nm with a field-of-view of about 15 μm in diameter. Even higher resolution will enable quantifications of microstructure and grain-to-grain interactions under pressure, density determinations of amorphous/liquid materials, and phase transition. Recently, high resolution imaging microscopy has been applied to study the equations of state and phase transition of tin at HP (Wang et al. 2012).

Full-field imaging method has been applied for X-ray microtomography based on X-ray absorption. By rotating an opposed anvil device under load, radiographic images of a sample projected in a plane parallel to the loading/rotating axis can be collected at small angular intervals at HP and HT in the same way as conventional absorption-based micro-tomography (Wang et al. 2005b). The setup at 13-BM-D of the APS allows both Drickamer and torroidal anvil cells to be used in a 250 ton press, with a Si(111) monochromator tunable between 5 and 65 keV. This technique has been used for measuring volume of amorphous material for equation of state determination (Lesher et al. 2009) and 3D microstructure of composite materials under shear deformation (Wang et al. 2011). Similar apparatus have since been developed at Spring-8 (Urakawa et al. 2010) and ESRF (Alvarez-Murga 2012).

Other HP X-ray imaging techniques are being developed. There are growing activities in HP coherent diffraction imaging (HP CDI) experiments. HP CDI provides information on shapes of a nano-crystal and its internal 3D strain distributions (Pfeifer et al. 2006; Le Bolloch et al. 2009; Yang et al. 2013). X-ray topography provides information of internal strain and defects of crystals. There is no HP topography work reported so far. However, X-ray topography images are used for selecting diamond anvils (Dewaele et al. 2006) and improving the synthetic procedures in diamond crystal growth in the CVD process at Carnegie Institution of Washington.

Time resolved X-ray techniques at HP. Time resolved HP studies can provide important information on structural dynamics, phase transition kinetics, chemical reactions under HP, and materials metastability and local minimum energy configurations. Because of small samples under HP, typical time resolution is still limited to a few seconds to minutes, numerous examples can be found in studies of CO_2 sequestration rate at HP with different initial conditions (Mckelvy et al. 2004), rheology of minerals under stress at mantle pressures (Wenk et al. 2004), the post-spinel transition in Mg_2SiO_4 (Kubo et al. 2002), and HP melting temperature determination. Recently with the use of Pilatus detectors, a time resolution of 30 μs has been reached in a HP XRD study of phase transition in a Ni-Fe alloy (Yoo et al. 2011). With an intensified CCD, single crystal diffraction spots have been collected with a single pulse of beam at the APS (70 ps width with 153 ns between pulses) in dynamic shockwave experiments (Turneaure et al. 2009; Luo et al. 2012).

Because synchrotron radiation is a pulsed source with a well-defined timing structure, pump/probe experiments can be also applied besides single-shot experiments. For example, pulsed laser heating can be synchronized with X-ray beam pulses for thermal equations of state measurements (Goncharov 2010; Yoo et al. 2011). Pulsed internally-heated DAC may also be applied for more spatially uniform heating. Dynamic diamond anvil cell (dDAC) (Evans et al. 2007) may be coupled with synchrotron pulses for studying phase transition kinetics

and behaviors of metastable phases. Pulsed magnetic field may be integrated with HP X-ray techniques for studying strongly correlated systems.

While XRD will still remain the primary technique for developing time resolved measurements, other HP X-ray techniques (SAXS, XAS, XES, NFS, radiography, etc.) may be applied for time-resolved measurements at HP. Energy dispersive XAS (Pascarelli and Mathon 2010), for example, has been applied in time-resolved HP XAS measurements at a spatial resolution at ~20 μm level. X-ray radiography and Laue diffraction have been applied for imaging the shock front in dynamic compression experiments (Jensen et al. 2012; Luo et al. 2012).

New FEL sources will provide coherent X-ray beams of extremely high flux in a pulse-duration of sub-ps. The high flux in a single pulse (~10^{12} photons) will be sufficient for single pulse XRD experiment, and will enable HP spectroscopy measurements in time-resolved manner. Besides FELs, short pulse X-rays are generated by high power laser facilities (such as OMEGA and NIF). Such short pulsed X-rays have been used for radiography and XRD measurements in dynamic shock experiments (Lee et al. 2006; Brygoo et al. 2007).

HIGH PRESSURE TECHNIQUES INTEGRATED WITH SYNCHROTRON RADIATION

The large volume press (LVP)

Several review articles have described the LVP techniques at synchrotrons (e.g., Vaughan 1993; Wang et al. 2002a; Wang 2010). Recent technical developments and science highlights at various beamlines are reviewed by several papers (e.g., Utsumi et al. 1998; Wang et al. 2009; Mezouar 2010). Here we only provide a brief summary.

Types of LVP used at synchrotron sources. The first is the well-known cubic-anvil, or DIA apparatus (Osugi et al. 1964), which consists of upper and lower pyramidal guide blocks, four trapezoid thrust blocks, and six square-tipped anvils, as illustrated in Figure 7. A ram force applied along the vertical axis is decomposed, by the 45° sliding surfaces, into three pairs acting along orthogonal directions, forcing the six anvils to advance (retract) synchronously towards (away from) the center of the cubic cavity, where the sample assembly is located. X-ray access is through vertical gaps between the side anvils. The diffraction vector is vertical, with possible 2θ angles up to about 25°.

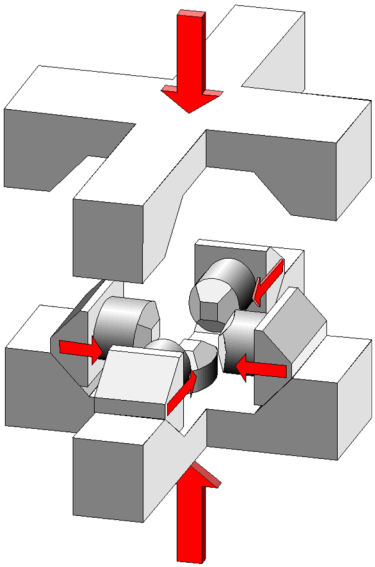

Figure 7. Conceptual diagram illustrating the principles of the DIA cubic anvil apparatus.

The second is the Kawai-type apparatus, which consists of a first-stage hardened steel cylinder cut into six parts, each having the inner tip truncated into a square surface, enclosing a cubic cavity, with the [111] axis of the cube along the ram load direction. Inside the cubic cavity is a second-stage assembly (referred to as the Kawai cell), which consists of eight WC cubes separated by spacers. Each cube has one corner truncated into a triangular face, so the eight truncated cubic anvils form an octahedral cavity in which the pressure medium is compressed. At beamline 13-ID-D of the APS (GSECARS), a Kawai-type module is used to compress 25 mm edge-length WC cubic

anvils. Diffracted X-rays pass through the gaps between the second-stage cubic anvils in a plane inclined at an angle of 35.264° from the loading direction. Conical access notches are made in the first-stage wedges, to allow a range of 2θ angles up to ~10° (Fig. 8).

The third is a hybrid system using a set of large DIA anvils to compress the Kawai cell (Anderson 1973). For convenience, we will refer this as the 6-8 Kawai type. The first such configuration was developed at the Photon Factory (Ohtani et al. 1989; Shimomura et al. 1992). Subsequently larger systems were adopted at SPring-8 (Utsumi et al. 1998). Figure 9 shows the apparatus at the insertion device beamline 13-ID-D at the APS (GSECARS). In this configuration hydraulic load is parallel to the [100] direction of the Kawai cell, and X-ray access is through

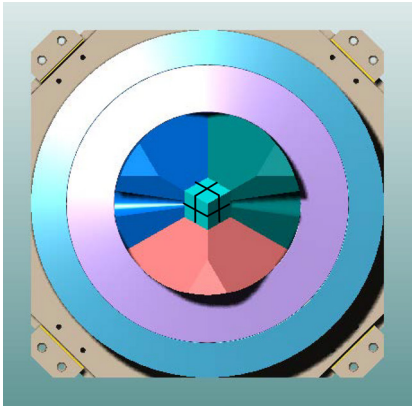

Figure 8. Top view of the T-25 module at GSECARS. The geometry is identical to Kawai-type systems used in most high-pressure laboratories, with the [111] axis of the eight-cube assembly along the loading axis. X-ray diffraction is through the gaps between WC anvils, inclined from the loading axis at 35.26°.

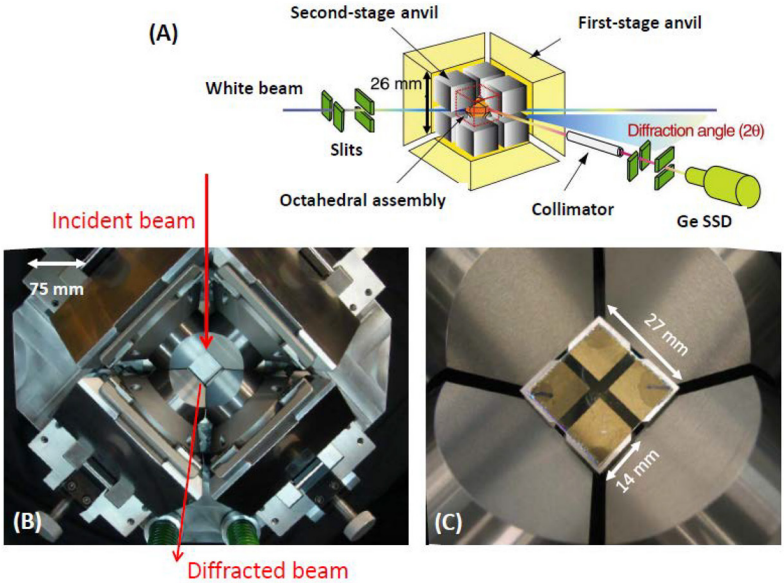

Figure 9. DDIA-30, a dual-purpose LVP for 1000 ton press at 13-ID-D of the APS. (A) Isometric view of the key components and setup (modified after SPring-8 website). (B) top view of the lower guide block showing first stage anvils and beam path. This configuration can be used as a DIA apparatus and a D-DIA for controlled deformation experiments. (C) Close-up of the second-stage cubic anvil arrangement (top view). This configuration allows HP of 50 GPa and 2000 K to be reached routinely.

horizontal anvil gaps when WC cubes are used as second-stage anvils. Notches are made in the first-stage DIA anvils to allow X-ray access. This apparatus is the most successful in generating "ultrahigh" pressures towards megabar using sintered diamond anvils, (e.g., Tange et al. 2008; Ito et al. 2010).

A new type of multi-anvil device was developed at the Institute for Study of Earth's Interior, Okayama University, Japan. This apparatus has a DIA-like geometry, but with each of the six anvils independently controlled by a hydraulic system (Ito et al. 2009). This configuration may add greater flexibility to the system by imposing desired hydrostatic or non-hydrostatic conditions. It is argued that the alignment of the six outer–stage anvils will also improve significantly, thus making it possible to compress the Kawai-cell with greater degree of accuracy, generating higher pressures with advanced anvil materials such as sintered diamond. A second 6-axis apparatus has been installed at Bayreuth Institute of Geosciences (Manthilake et al. 2012). Although no such systems have been used at synchrotron beamlines yet, a similar apparatus has been installed at the neutron PLANET beamline at Japan Photon Accelerator Research Complex (J-PARC; J-PARC Newsletter, No. 49, July 2012).

Not all LVPs are multi-anvil devices. The toroid anvil cell, first developed in the former Soviet Union (Khvostantsev 1977), operates on the principles of opposed anvils, similar to the DAC. Instead of flat anvil tips as in the DAC, toroid anvils have a half-spherical depression so that the two anvils enclose a semi-spherical cavity. One or several toroidal depressions are made concentric with the central sample cavity for preformed gaskets that are used to minimize extrusion (Fig. 10). Besson et al. (1992) integrated this device with a compact hydraulic system, allowing portability and great flexibility. The Paris-Edinburgh (PE) cells, as they are known now, are currently in use at many synchrotron and neutron sources. Sample size is typically in the millimeter range. X-ray access is through the gaps between the two anvils for synchrotron diffraction, where the largest diffraction angle is in the plane perpendicular to the loading axis. Hirth and Kohlstedt (2003) reviewed the HP activity at ESRF using a PE cell.

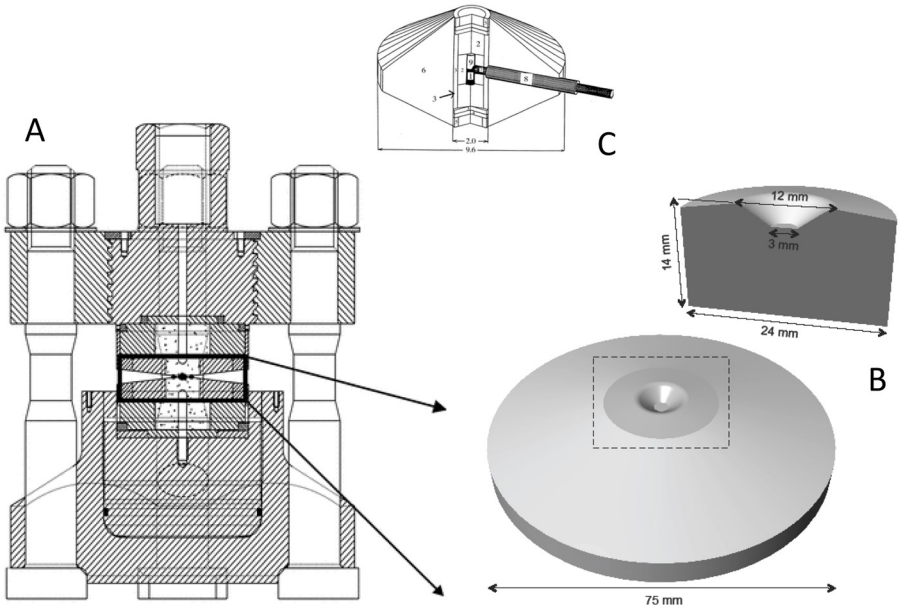

Figure 10. The Paris-Edinburgh cell. (A) Cross-section of the overall apparatus. (B) WC PE anvil, along with a cross section showing typical dimensions. (C) Schematic of a PE assembly.

The Drickamer cell is another widely used opposed anvil device (Balchan 1961) in which two large anvils (diameters 10 mm or above) with an optimal tapered angle are compressed inside a containment ring, typically made of WC or hardened steel, with X-ray access holes for diffraction (Fig. 11). Such devices have been used in Japan at synchrotrons (Yoshiasa et al. 1999; Gotou et al. 2006) for some time and are now used for a number of new applications, described below. Nishiyama et al. (2009) developed a modified Drickamer cell for HP deformation at HT using ADXRD. Another modified Drickamer anvil apparatus was developed by Gotou et al. (2011), where small depressions are introduced into the anvil tops, similar to the toroid anvils. This increases the height of the sample, allowing more uniform heating with slight decrease in pressure efficiency.

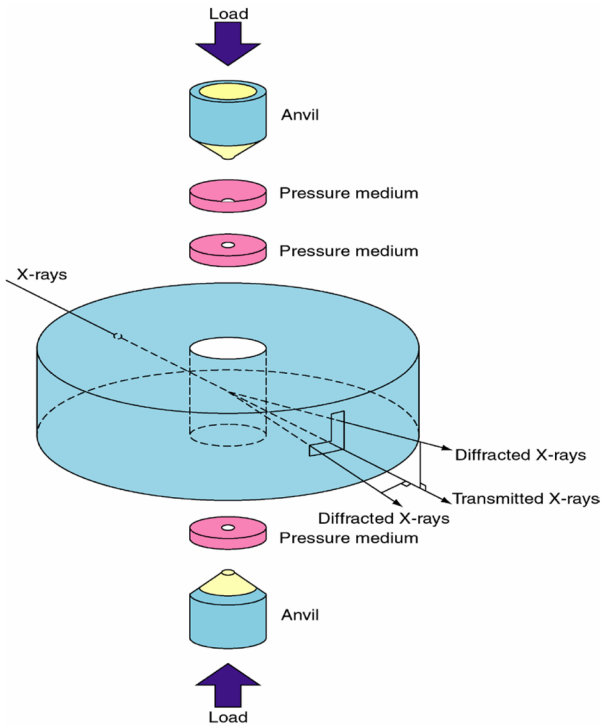

Figure 11. The Drickamer cell. With sintered diamond as anvil material, it can generate up to 30 GPa pressure, with a sample about 0.2-0.3 mm in linear dimensions.

Diffraction optics. When EDXRD is used in LVPs, it is essential to maintain fine beam collimation in order to minimize background scattering from the surrounding pressure media. This is achieved by using slits and collimators which are pairs of blades made of heavy metals (e.g., tungsten or tantalum alloys). Typical slit openings are on the order of 50 to 100 μm, defining a diffracting volume with the maximum linear dimensions about 1 mm. Cooling may be necessary especially for incident slits to minimize thermal drift caused by intense synchrotron radiation.

For ADXRD, collimation on the diffraction side is sometimes omitted. Instead, amorphous (e.g., B) and/or low scattering materials are inserted in the beam path serving as "windows". This technique works well with area detectors (CCD or image plates) when the sample has

sufficient scattering power so that contributions from the window materials are negligible. For weak scattering samples especially non-crystalline materials, Soller slits are necessary and have been used on the diffraction side (Yaoita 1997; Mezouar 2002; Morard 2011). These slits are multichannel collimators with two arrays of slits prefabricated to cover a given two-theta range, forming two concentric arches centered at the sample. By oscillating the two rows of slits slightly around the center of the sample, background scatter is eliminated, allowing clean diffraction signals from the sample to be recorded. This technique has been successfully applied to studying melt structures of Fe-(S, Si) alloys (Morard et al. 2007b, 2008).

Pressure temperature controls. Pressure is controlled by varying the hydraulic ram load, typically through proportional-integral-derivative (PID) feedback control logic, and measured based on the *P-V-T* equations of state of standard materials that are placed in close proximity of the sample. A comprehensive review on various pressure scales is provided by Decker et al. (1972). With positive displacement pumps (also known as syringe pumps) as load generators, extremely fine control can be achieved. Modern systems are automated for increasing and decreasing ram load, often with multiple cycles. However, ram load and sample pressure do not have a simple relation. The loading-unloading pressure "hysteresis loop" is primarily due to plastic deformation in the pressure media and gaskets. Fortunately, the hysteresis behavior is predictable for a given cell assembly. Pressure gradients in the sample are generally small when experiments are conducted properly (on the order of 0.1 GPa/mm or below), and ultimately controlled by the yield strengths of the sample and the surrounding pressure media. With increasing temperature (decreasing yield strength), pressure gradients diminish.

Temperature is generally generated by resistive heating and measured by a thermocouple. Many materials have been used as heaters, the most commonly used being graphite, noble metals, and certain ceramics (e.g. $LaCrO_3$) (Ohtani 1979). All of these materials have certain limitations. Graphite has limited pressure applicability due to its transition to diamond. Metals and $LaCrO_3$ attenuate X-rays thereby affecting diffraction signal, if used in the beam path. Recently, TiB_2 has been employed which is capable of generating temperatures in excess to 2500 K and to very high pressures (at least 50-60 GPa) (Arima et al. 2007). AC power supplies are preferred as DC supplies might generate a DC bias in the thermocouple signal, thereby causing erroneous temperature reading. PID control is commonly used for controlling heating rate and maintaining a constant temperature during data collection. Despite some attempts, the effect of pressure on thermocouple emf remains unclear. It appears that W/Re based thermocouples are the least affected by pressure effect (Ohtani 1979) and therefore the most commonly used.

Stress/strain control. Yamazaki and Karato (2001) constructed a rotational Drickamer apparatus (RDA). The pressure generation mechanism is based on the Drickamer cell, but with one of the anvils rotated under high *P* and *T*, generating large shear strains in the sample. Although stress and strain fields are heterogeneous throughout the sample, the large strain capability makes this a unique apparatus for studying plastic deformation and deformation-induced preferred orientation under high *P* and *T*.

The concept of deformation DIA (D-DIA) was first described by Wang et al. (1998). It is a modification of the DIA apparatus, with additional independent control of the displacement of one pair of anvils, provided by two additional hydraulic actuators, called differential rams (Wang et al. 2003). The differential rams are located within the guide blocks of the D-DIA module (Fig. 12) and react against the platens driven by the main hydraulic ram, which provides quasi-hydrostatic pressurization. The guide blocks not only support the forces confining the side wedges, they now have also become thick-walled pressure containers for the hydraulic fluid driving the differential rams.

When the differential rams are driven symmetrically, strain rates of 10^{-3} to 10^{-7} s^{-1} can be imposed on a sample several mm in length. The D-DIA is capable of shortening as well

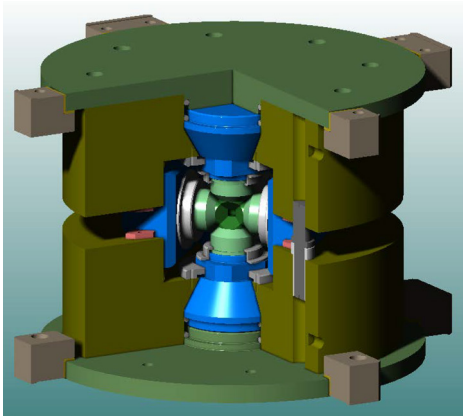

Figure 12. Cutaway view of the D-DIA with differential rams in the upper and lower guide blocks. Note locations of the differential rams. Modified after Wang et al. (2003).

lengthening the sample, making it possible to conduct stress-strain loops, a widely used method in conventional deformation studies. Deformation in simple shear, using 45°-cut pistons, is also used for much higher strains, at the cost of reducing sample volume (Ohuchi et al. 2010). By driving the differential rams cyclically, one creates a dynamic, sinusoidal stress boundary condition, which can be used to study a number of interesting phenomena at high *P* and *T* such as bulk attenuation in minerals (Li and Weidner 2008) and twin domain switching in ferroelastic materials (Li and Weidner 2010).

The D-DIA also has advantages in quasi-hydrostatic pressure generation. The differential rams make it possible to compensate elastic deformation in the high pressure apparatus at various loads. By adjusting the differential ram positions one can generate conditions closer to hydrostatic than a regular DIA. These advantages have inspired a new generation of multi-anvil systems. Large DDIA modules have been installed at LVP beamlines at SPring-8 (Kawazoe et al. 2011), ESRF, and the APS (Fig. 9) (Wang et al. 2010b).

Sample imaging. Synchrotron radiography has been used since the 1980's for measuring melt viscosity using the falling sphere technique (Kanzaki et al. 1987). Starting from the late 1990's the radiography technique was integrated into APS beamlines and used as an efficient way to visualize samples during LVP experiments (Wang et al. 2000). The technique has been adopted by virtually all LVP beamlines since then. Sample length measurements are routinely conducted in deformation studies and ultrasonic velocity measurements. Recently, this simple technique has been extended for measuring bulk attenuation (Li and Weidner 2008) with cyclic loading in the D-DIA, and for studying thermal diffusivity of minerals at high pressures (Dobson et al. 2010) with controlled sinusoidal temperature cycling.

Wang et al. (2005b) developed a high-pressure X-ray tomography imaging system. By using thrust bearings to support ram loads and high-torque gears, opposed anvil cells such as Drickamer or toroid anvil devices can have unlimited rotation with respect to the loading axis. X-rays that pass through such a rotation anvil apparatus (RAA) are converted into visible light using a scintillating screen. Absorption contrast through the sample and pressure media are recorded at various angles as radiographs, which are then processed to reconstruct three-dimensional tomographic images. With parallel beam imaging, spatial resolutions of 2-3 microns are achievable, making this device a powerful tool for observing 3D microstructure under high *P* and *T*. This technique has been used to measure density of molten material under high *P* and *T* (Lesher et al. 2009), investigate liquid-liquid surface tension (Terasaki et al. 2008), examine shear-induced fabric transition in multiphase composites (Wang et al. 2011), and study segregation process of molten Fe from silicate matrix for a better understanding

of the core formation processes in the Earth's early history (Chen et al. 2011). Other HP tomography techniques have since been developed at SPring-8 (Urakawa et al. 2010) and ESRF (Alvarez-Murga 2012).

Ultrasonic measurements. The large sample volume in the LVP allows one to measure acoustic wave velocities on polycrystalline and single crystals at high *P* and *T*. Synchrotron radiation with ultrasonic travel time determination offers a unique combination as sample length (which is needed to convert travel times to velocities) and density can be determined by radiography and diffraction, respectively. The reader is referred to other reviews for technical details (e.g., Li et al. 2004a; Li and Liebermann 2007). With the advanced instruments travel times of a 0.5 mm long sample can be determined accurately. This means that the technique can be applied to quite high pressures (in excess to 50 GPa). The simultaneously measured *P*-*V*-*T* (through X-ray diffraction), sample length (X-ray imaging), and acoustic travel times (ultrasonic interferometry) informative has allowed establishment of redundant equations of state, making it possible to examine closely precision and accuracy of diffraction-based pressure standards (e.g., Kono et al. 2009).

Acoustic emission (AE) techniques have been integrated with deformation in the D-DIA after successful development in the DIA apparatus at DESY (Gasc et al. 2011). By mounting acoustic transducers on the back side of all six anvils, AE events can be monitored throughout deformation process. Thanks to the development of advanced electronics and software, continuous recording of AE events allows microseismology to be performed in the laboratory. Effects of phase transformation from olivine to spinel on faulting in polycrystalline Mg_2GeO_4 samples have been investigated (Schubnel et al. 2013).

Diamond anvil cell techniques

The extreme hardness and strength of diamond allows generation of very high pressures reaching conditions corresponding to the center of the Earth (Mao et al. 1990; Akahama and Kawamura 2007; Dubrovinsky et al. 2012). Because of its transparency to much of the electromagnetic spectrum, including high energy X-rays above 10 keV and low energy ultraviolet-visible-infrared radiation below 5 eV, numerous diffraction, scattering, and absorption probes can be employed for determination of electronic, dynamic, and structural properties of samples under pressure. This transparency also allows for utilizing laser beams that can heat samples up to temperatures over 4000 K while at extreme pressures (Ming and Bassett 1974; Boehler et al. 1990; Shen et al. 2001).

Pressure generation. The DAC design is based on Bridgman's original idea in which the sample is placed between the polished culets of two diamonds and is contained by a gasket (Fig. 13). Since pressure is force divided by area, extreme pressures can be generated by opposing anvils with small culet sizes.

A number of different cell designs have been developed for various applications. To ensure precise alignment for small culets in ultra-high pressure generation, a long piston cylinder design (such as the Mao-Bell type) is often used. Symmetrical design is suitable for double sided laser heating experiments (Shen et al. 1996; Mao et al. 1998a). Special DACs have been designed for externally resistive heating techniques (Fei and Mao 1994; Bassett et al. 2000; Dubrovinsky et al. 2000). For magnetic measurements, non-magnetic alloys (such as Cu-Be alloy) are used for the cell body. The panoramic cell has been developed (Mao et al. 2001), which provides wide opening in the radial direction and is widely used in HP spectroscopy experiments. The recently developed plate cell (Boehler 2006) removed the need of guiding alignment, making the cell even more compact, with wide opening in both radial and axial directions (Fig. 14).

Many new developments have been made on the designs of diamond anvils to meet the needs of various measurements. The Boehler-Almax anvil design (Boehler 2006) (Fig.

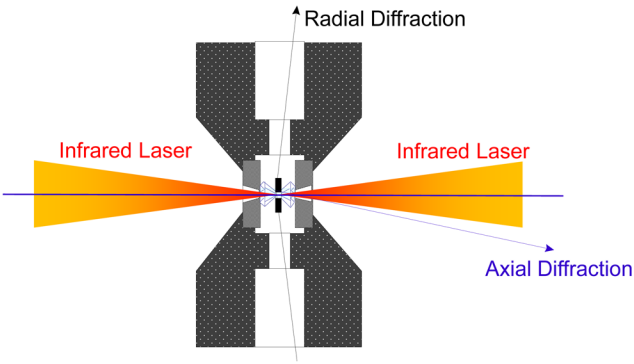

Figure 13. Schematic of a symmetrical diamond anvil cell. X-ray access may be applied in both axial and radial directions. Pressure is generated by pressing two diamond anvils with small culets.

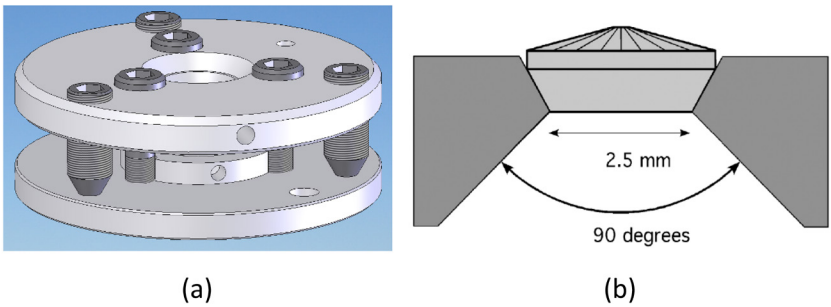

Figure 14. (a) The plate cell design; (b) large aperture diamond anvil with tungsten carbide support from the side, making the X-ray opening of more than 80 degrees. Modified after Boehler (2006).

14) provides large opening access (> 90°) along the loading axis, and is widely used in HP XRD, in particular in HP single crystal XRD. Fully or partially perforated anvils have been used to gain penetration power for low energy X-rays in HP XAS, HP XMCD, and HP PYF spectroscopy experiments. Use of partially perforated anvils can significantly reduce scattering from anvil materials, effectively minimizing Compton scattering from anvils in experiments of amorphous or liquid materials with high X-ray energy. With focused ion beam (FIB) and other micro-engineering techniques, small holes and/or grooves may be made for containing samples or to reduce the X-ray path length. For example, the so-called "holy" and "groovy" anvils are used in HP XAS experiments with hydrothermal DAC (Bassett et al. 2000; Mayanovic et al. 2007b). Electrical leads and magnetic coils may be implemented at the tip of anvils (Jackson et al. 2003), and when combined with HP synchrotron measurements, complementary information may be obtained (Uhoya et al. 2012).

The maximum pressure with the single stage type DAC is in the vicinity of 400 GPa (Akahama and Kawamura 2010). For generating pressures of 500 GPa and above, new anvil designs together with smaller probing beams (< 1 μm) are needed. Efforts are being made to optimize the anvil shape using the fine-element calculations. Recently, pressures as high as 600 GPa have been reached by a double stage mechanism, i.e., inserting a small pairs of anvils inside the sample chamber between diamond anvils (Dubrovinsky et al. 2012). Higher pressures may be reached when the double stage DAC is combined with fast ramping loading and time-resolved measurements.

Hard metals, such as stainless steels and rhenium, are often used as gasket materials. These metals are of high ductility and easy to machine and handle. For X-ray access in the radial direction, low-Z materials (Be, B, cBN, diamond powder) are used as gasket or insert materials in the sample chamber. Hydrostatic pressure can be generated in the DAC when a proper medium is used. Methanol-ethanol mixture, silicone oil, and noble gases such as helium and neon are few commonly used examples. However, above 11 GPa at room temperature, all known fluids solidify and develop nonhydrostatic stresses proportional to their strength. Above 20 GPa, even the weak noble gas solids, argon and neon, show non-hydrostaticity. Helium, solidified at 11 GPa at room temperature (Pinceaux et al. 1979), is considered to be the best pressure medium, which provides hydrostatic pressure up to 11 GPa, and good quasi-hydrostatic pressure condition up to 50 GPa due to its low shear strength (Takemura 2001). Quantifying the deviatoric stress under uniaxial compression has been made by HP XRD (Meng et al. 1993) and by monitoring the 3-dimensional lattice strains with radial XRD (Mao et al. 1998b).

Temperature techniques. HP DAC experiments can be combined with temperature techniques from a few degrees to thousands of degrees in Kelvin. DACs can be inserted in cryostats and cooled down to below 4 K. Various cryostats have been developed for accommodating different cells and different measurement geometry (Fig. 15).

There are two major resistive heating methods—external and internal. External furnaces provide accurate and well-controlled temperature conditions. There is an intrinsic temperature limit, however, due to rapid graphitization of diamond above 1900 K, even in an inert environment and vacuum (Seal 1963). The entire DAC may be heated by a resistively heated furnace up to 700 K. For higher temperatures, a small heater around diamond anvils may be used for temperatures up to 1200K (Fei and Mao 1994). With a graphite heater around diamond culets, temperatures as high as 1700 K have been reported with resistive heating methods (Dubrovinsky et al. 2000). Due to softening of the stress-bearing components, including the sample gasket, the diamond seat, and the diamond anvil itself, maximum attainable pressure is limited. The internally heated method, on the other hand, locally heats the sample in the chamber. Often, the sample itself is used as a conductive object and heating is applied electrically (Boehler 1986). Zha and Bassett (2003) used rhenium ribbon as a heating object and the sample was placed in a hole in the ribbon. Temperatures may be reached as high

Figure 15. Examples of cryostats at sector 16 (HPCAT) at APS.

as the melting temperatures of the conductors. By the chemical vapor deposition method, a resistively heated wire circuit may be built in the diamond anvil culet, this may increase the maximum pressure attainable.

The transparency of diamond allows application of near- and mid-infrared lasers (CO_2, Nd:YAG, Nd:YLF) to heat samples between two diamond anvils at high pressures (Ming and Bassett 1974). Regarding the temperature range, there is no high temperature limit with this technique in principle. The challenging part is to control and measure them accurately and to characterize the sample at defined conditions. The temperature measurement is based on spectral pyrometry. By measuring the thermal radiation from the hot sample over a wavelength range, temperatures can be calculated by fitting the radiation to Planck's equation (Boehler 1986; Heinz and Jeanloz 1987). A double sided laser heating system (Shen et al. 1996) was introduced for the minimization of temperature gradients radially and axially in a laser heated sample. Thanks to the micro X-ray beam size which improved the spatial resolution and ensured that the X-ray beam size is significantly smaller than the laser heated spot. Many synchrotron facilities have equipped with double sided laser heating systems. The laser heated DAC experiments become a routine capability in HP XRD and HP spectroscopy. Recently, portable laser heating systems have been developed (Boehler et al. 2009; Dubrovinsky et al. 2009; Shen et al. 2010), which will lead to more use of the laser heating technique in specialized beamlines with various X-ray probes.

Pressure controls and measurements. The compact design of DAC allows for pressure control by just turning screws manually. This makes the DAC device portable and applicable in many probing techniques. To gain precision in pressure control and to access remotely when contained in other equipment such as cryostats, furnaces, and magnets, the diaphragm design (sometimes referred to membrane control) using compressed gas has been developed (Daniels and Ryschkewitsch 1983), and now widely used in synchrotron facilities. By regulating the compressed gas (e.g., He-gas) pressure, the force applied to the anvils may be controlled precisely and fine pressure change can be made. Recently, motor driven gear boxes have been developed for controlling the screw turns, providing remote precise pressure controls. With these remote control devices, either by mechanical gear box or by diaphragm, X-ray measurements with small pressure increment become possible, revealing subtle changes in compression and unusual phenomena close to phase transitions.

Using the pressure-volume equations of state data of well-studied materials (e.g., MgO, NaCl, Au, W), pressures can be determined by measuring the volumes of these standard materials by HP XRD. Pressure can also be determined by optical methods, e.g., using the ruby fluorescence (Mao et al. 1986) and Raman peaks of diamond (Akahama and Kawamura 2010). Pressure determination at HT is challenging because of the lack of accurate data of pressure-volume-temperature equations of state. Nevertheless, attempts have been made to construct internally-consistent data set with available X-ray and optical techniques (Sinogeikin et al. 2006; Fei et al. 2007; Komabayashi and Fei 2010). In addition, weakly temperature dependent sensors, e.g., YAG:Sm (Zhao et al. 1998), have been developed for pressure determination at HT. It should be mentioned that establishing a reliable pressure scale remains as one of the most important goals in high pressure mineral physics.

Dynamic shockwave techniques

In shock wave experiments, the sample is subjected to HP and HT by dynamic processes. A shock wave is driven through the sample by means of an explosive charge, by the collision of a flying object, or by high power lasers. Compared to the projectile technique, the laser shock technique can yield very high amplitude pressure loadings (as high as 50 TPa) with very short durations (in fs). The DAC may be integrated with the laser-driven shock (Celliers et al. 2010; Loubeyre et al. 2004). By controlling the ramp rate, these experiments (Smith et

al. 2007) can provide single shot equation-of-state data close to the isentrope, information on the kinetics of phase transformations, and material strength at high pressures. A number of techniques have been developed to measure the velocity of shock wave and the velocity to which the sample material has been accelerated. These measurements allow us to derive the density and pressure of the sample under loading (Brown and McQueen 1982).

Recently, X-ray techniques have been applied in shockwave experiments at synchrotron facilities and other high power laser facilities (OMEGA, NIF). Single crystal XRD has been used for studying the deformation of materials under shock (Turneaure et al. 2009). The shock front can be monitored by X-ray radiography (Ping et al. 2011). Dynamic response of materials under shock has been measured by using the phase contrast imaging technique (Jensen et al. 2012). Using the X-ray white Laue technique, the shock wave propagation can be recorded by using the timing structure of synchrotron pulses (Suggit et al. 2010; Luo et al. 2012).

A BRIEF OUTLOOK

Expanding *P-T* range

The accessible pressure range ultimately defines the scope of HP research. In the past two decades, the number of publications from the HP synchrotron research has increased exponentially, thanks to the micro-sized (2-5 μm) synchrotron probes and new high pressure techniques. However, the highest pressure has reached a plateau at ~400 GPa (Akahama and Kawamura 2010) with the single stage type DAC. Recently, with a double stage DAC configuration, pressures up to 600 GPa have been reached in a much smaller sample volume (Dubrovinsky et al. 2012). Nano-XRD probes at synchrotron facilities therefore provide spatial resolution required for studying materials at extreme conditions with very small volume. Together with the developments in X-ray optics, ultra-stable sample stages, and advanced detectors, even higher pressures reaching 1 TPa and beyond may be feasible in the near future in the static DAC experiments. The nano-probes may be combined with dynamic DAC (d-DAC) (Evans et al. 2007), which may enable time resolved experiments at increasingly broader pressures and even more extreme temperature conditions before the anvil's failure. The nano-probes can also be applied in less homogeneous samples, or in precise single-crystal studies of individual crystallites within a powder sample.

Pressure and temperature ranges are also constantly expanding for the LVP. Using sintered diamond as second-stage anvils, the 6-8 type Kawai apparatus are approaching the megabar mark (Ito et al. 2010). With a pair of advanced nano-polycrystalline diamond as third-stage anvils (Irifune et al. 2003) in the octahedral pressure medium in the 6-8 Kawai apparatus (the so-called 6-8-2 configuration), Kunimoto and Irifune (2010) reported a pressure of 125 GPa up to 1100 K. Under these conditions the sample dimensions are about 100-200 microns in linear dimensions.

New HP synchrotron techniques

Various new types of DACs are being developed for ultra-high pressure, large opening, or compactness to fit in the varieties of X-ray measurements. Portable systems, including laser heating systems, optical Raman and ruby fluorescence systems, and microfocusing mirrors, have been developed and are being integrated at many beamlines. Rather than concentrating on HP beamlines, this approach takes advantages of specialized beamlines with well-developed X-ray techniques. Many new HP synchrotron techniques are being developed in XRD, XRS, and IXS, in particular in the areas of imaging techniques and time-resolved measurements.

Imaging capabilities (coherent diffraction imaging, mass density tomography, full field imaging) are being actively integrated with DAC for HP studies with resolutions from 1 μm down to 30 nm, which will open a new era of imaging HP phases, for studying the plasticity,

elasticity, and precise equations of state of amorphous/liquid materials. Imaging in the LVP has received much attention recently. Both radiography and tomography techniques will be used more intelligently. Attenuation and thermal conductivity are just recent examples of new applications for radiography. With advanced tomography techniques, high pressure tomography will see much improved mechanical and optical components, to allow 3D microstructure imaging to the sub-micron level in spatial resolution. Diffraction tomography may be applied, allowing grain-to-grain examination of a bulk sample under high *P* and *T*.

A beamline dedicated to dynamics compression science is under construction at APS for time-resolved studies in dynamic processes and would be the first of its kind at a third-generation high-energy synchrotron facility. Dynamic compression capabilities (utilizing high-velocity impacts, high-intensity lasers, and pulsed power generators), coupled with ultra-fast measurements at the APS, represent the most versatile approach for achieving the widest range of thermo-mechanical conditions in a controlled manner.

Because HP samples are always embedded in surrounding materials (anvils, gaskets, pressure media), excellent collimation is required to remove signals from surrounding materials. Developments for precise collimation down to micron size for various HP spectroscopy techniques are important and will effectively increase the signal-to-noise ratios. Spectroscopy in the LVP is an area that may see huge advances in the future. With more brilliant synchrotron radiation, a wider range of photon energies will be measureable through pressure media, allowing many techniques that currently can only be used in the DAC to be applied to the LVP. Since LVP is capable of stable and uniform *P* and *T* conditions, HT spectroscopy may be applied to minerals under conditions more representative to the Earth and planetary interiors.

ACKNOWLEDGMENTS

Thanks are due to Ligang Bai, Daijo Ikuta, and Yuming Xiao for their help in preparation of this manuscript. Mark Rivers is thanked for Figure 2. HPCAT is supported by DOE-NNSA under Award No. DE-NA0001974 and DOE-BES under Award No. DE-FG02-99ER45775, with partial instrumentation funding by NSF. GeoSoilEnviroCARS (GSECARS) is supported by the National Science Foundation - Earth Sciences (EAR-0622171) and Department of Energy - Geosciences (DE-FG02-94ER14466). APS is supported by DOE-BES, under Contract No. DE-AC02-06CH11357. YW thanks continuing NSF support for LVP developments at GSECARS (EAR-0001088, 0652574, 0711057, 0968456, and 1214376).

REFERENCES

Akahama Y, Kawamura H (2007) Diamond anvil Raman gauge in multimegabar pressure range. High Pressure Res 27(4):473-482, doi: 10.1080/08957950701659544

Akahama Y, Kawamura H (2010) Pressure calibration of diamond anvil Raman gauge to 410 GPa. J Phys 215: 012195

Alvarez-Murga M (2012) In situ microdiffraction and microtomography of heterogeneous high-pressure high-temperature forms of C_{60}. Ph.D. thesis, ESRF, Grenoble

Anderson OL (1973) Comments on the power law representation of Birch's Law. J Geophys Res 78(23):4901-4914, doi: 10.1029/JB078i023p04901

Andrault D, Munoz M, Bolfan-Casanova N, Guignot N, Perrillat J-P, Aquilanti G, Pascarelli S (2010) Experimental evidence for perovskite and post-perovskite coexistence throughout the whole D″ region. Earth Planet Sci Lett 293:90-96

Antonangeli D, Siebert J, Badro J, Farber DL, Fiquet G, Morard G, Ryerson FJ (2010) Composition of the Earth's inner core from high-pressure sound velocity measurements in Fe–Ni–Si alloys. Earth Planet Sci Lett 295(1-2):292-296, doi: 10.1016/j.epsl.2010.04.018

Antonangeli D, Siebert J, Aracne CM, Farber DL, Bosak A, Hoesch M, Krisch M, Ryerson FJ, Fiquet G, Badro J (2011) Spin crossover in ferropericlase at high pressure: a seismologically transparent transition? Science 331(6013):64-67, doi: 10.1126/science.1198429

Aquilanti G, Pascarelli S, Mathon O, Munoz M, Narygina O, Dubrovinsky L (2009) Development of micro-XANES mapping in the diamond anvil cell. J Synchrotron Radiat 16:376-379, doi: 10.1107/s0909049509007134

Arima H, Ohtaka O, Hattori T, Katayama Y, Utsumi W, Yoshiasa A (2007) In situ XAFS and XRD studies of pressure-induced local structural change in liquid AgI. J Phys Condens Matter 19(7):076104

Badro J, Fiquet G, Guyot F, Rueff J-P, Struzhkin VV, Vanko G, Monaco G (2003) Iron partitioning in Earth's mantle: toward a deep lower mantle discontinuity. Science 300(5620):789-791

Balchan AS, Drickamer HG (1961) High pressure electrical resistance cell, and calibration points above 100 kbars. Rev Scic Instrum 32:309-313

Ballirano P, Caminiti R (2001) Reitveld refinements on laboratory energy dispersive X-ray diffraction (EDXD) data. J Appl Crystallogr 34:757-762

Bassett WA, Reichmann H-J, Angel RJ, Spetzler H, Smyth JR (2000) New diamond anvil cells for gigahertz ultrasonic interferometry and X-ray diffraction. Am Mineral 85:283-287

Besson JM, Nelmes RJ, Hamel G, Loveday JS, Weill G, Hull S (1992) Neutron powder diffraction above 10 GPa. Physica B 180-181(Part 2):907-910

Boehler R (1986) The phase diagram of iron to 430 kbar. Geophy Res Lett 13: 1153-1156

Boehler R (2006) New diamond cell for single-crystal X-ray diffraction. Rev Sci Instrum 77(11):115103, doi: 10.1063/1.2372734

Boehler R, Von Bargen N, Chopelas A (1990) Melting, thermal expansion, and phase transitions of iron at high pressures. J Geophys Res 95:21,731-21,736

Boehler R, Musshoff HG, Ditz R, Aquilanti G, Trapananti A (2009) Portable laser-heating stand for synchrotron applications. Rev Sci Instrum 80(4):045103

Bradley JA, Moore KT, Lipp MJ, Mattern BA, Pacold JI, Seidler GT, Chow P, Rod E, Xiao Y, Evans WJ (2012) 4f electron delocalization and volume collapse in praseodymium metal. Phys Rev B 85(10):00102

Brygoo S, Henry E, Loubeyre P, Eggert J, Koenig M, Loupias B, Benuzzi-Mounaix A, Rabec Le Gloahec M (2007) Laser-shock compression of diamond and evidence of a negative-slope melting curve. Nat Mater 6(4): 274-277, doi: 10.1038/nmat1863

Buras B, Olsen JS, Gerward L (1976) X-ray energy-dispersive powder diffractometry using synchrotron radiation. Nucl Instrum Methods 135(1):193-195, doi: 10.1016/0029-554x(76)90845-4

Cainrs RJR, Ottewill RH, Osmond DWJ, Wagstraff I (1976) Studies on the preparation and properties of latices in nonpolar media. J Colloid Interface Sci 54(1):45-51

Catalli K, Shim S-H, Prakapenka VB, Zhao J, Sturhahn W (2011) X-ray diffraction and Mössbauer spectroscopy of Fe^{3+}-bearing Mg-silicate post-perovskite at 128–138 GPa. Am Mineral 95(2-3):418-421, doi: 10.2138/am.2010.3352

Celliers PM, Loubeyre P, Eggert JH, Brygoo S, Mcwilliams RS, Hicks DG, Boehly TR, Jeanloz R, Collins GW (2010) Insulator-to-conducting transition in dense fluid helium. Phys Rev Lett 104(18), doi: 10.1103/PhysRevLett.104.184503

Chapman KW, Chupas PJ, Halder GJ, Hriljac JA, Kurtz C, Greve BK, Ruschman CJ, and Wilkinson AP (2010) Optimizing high-pressure pair distribution function measurements in diamond anvil cells. J Appl Crystallogr 43: 297-307, doi: 10.1107/s0021889810002050

Chen B, Zhang D, Leng W, Jackson JM, Wang Y, Yu T, Liu J, Li J (2011) Rapid terrestrial core formation from in situ X-ray computed microtomography. American Geophysical Union, Fall Meeting 2011, abstract #MR42A-02}

Chen B, Jackson JM, Zhao J, Wicks JK, Murphy CA (2012) Spin crossover equation of state and sound velocities of $(Mg_{0.65}Fe_{0.35})O$ ferropericlase to 140 GPa. J Geophys Res 117: B08208

Chen J, Wang Y, Duffy TS, Shen G, Dobrzhinetskaya LF (2005) Advances in High-pressure Technology for Geophysical Applications. Elsevier

Coppari F, Di Ciacco A, Filipponi A, Trapananti A, Agquilanti G, De Panfilis S (2008) Local structure of liquid and undercooled liquid Cu probed by X-ray absorption spectroscopy. J Physics Conference Series 121:042009, doi: 10.1088/1742-6596/121/4/042009

Daniels WB, Ryschkewitsch MG (1983) Simple double diaphragm press for diamond anvil cells at low-temperatures. Rev Sci Instrum 54(1):115-116, doi: 10.1063/1.1137223

Deb SK, Wilding M, Somayazulu M, Mcmillan PF (2001) Pressure-induced amorphization and an amorphous-amorphous transition in densified porous silicon. Nature 414:528-530

Decker DL, Bassett WA, Merrill L, Hall HT, Barnett JD (1972) High pressure calibration: a critical review. J Phys Chem Ref Data 1:1-79

Dewaele A, Loubeyre P, Andre R, Hartwig J (2006) An X-ray topographic study of diamond anvils: Correlation between defects and helium diffusion. J Appl Phys 99(10):104906, doi: 10.1063/1.2197265

Dewaele A, Mezouar M, Guignot N, Loubeyre P (2010) High melting points of tantalum in a laser-heated diamond anvil cell. Phys Rev Lett 104(25):255701, doi: 10.1103/PhysRevLett.104.255701

Ding Y, Haskel D, Ovchinnikov SG, Tseng Y-C, Orlov YS, Lang JC, Mao HK (2008) Novel pressure-induced magnetic transition in magnetite (Fe_3O_4). Phys Rev Lett 100:045508

Dobson DP, Hunt SA, Mccormack R, Lord OT, Weidner DJ, Li L, Walker AM (2010) Thermal diffusivity of MORB-composition rocks to 15 GPa: implications for triggering of deep seismicity. High Pressure Res 30(3):406-414

Dubrovinsky L, Saxena SK, Tutti F, Rekhi S, and Lebehan T (2000) In situ X-Ray study of thermal expansion and phase transition of iron at multimegabar pressure. Phys Rev Lett 84(8):1720-1723

Dubrovinsky L, Glazyrin K, McCammon C, Narygina O, Greenberg E, Ubelhack S, Chumakov AI, Pascarelli S, Prakapenka V, Bock J, Dubrovinskaia N (2009) Portable laser-heating system for diamond anvil cells. J Synchrotron Radiat 16:737-741, doi: 10.1107/s0909049509039065

Dubrovinsky L, Dubrovinskaia N, Prakapenka VB, Abakumov AM (2012) Implementation of micro-ball nanodiamond anvils for high-pressure studies above 6 Mbar. Nat Commun 3:1163, doi: 10.1038/ncomms2160

Duffy TS (2005) Synchrotron facilities and the study of the Earth's deep interior. Rep Prog Phys 68:1811-1859, doi: 10.1088/0034-4885/68/8/R03

Eggert JH, Weck G, Loubeyre P, Mezouar M (2002) Quantitative structure factor and density measurements of high-pressure fluids in diamond anvil cells by X-ray diffraction: Argon and water. Phys Rev B 65:174105

Evans WJ, Yoo C-S, Lee GW, Cynn H, Lipp MJ, Visbeck K (2007) Dynamic diamond anvil cell (dDAC): A novel device for studying the dynamic-pressure properties of materials. Rev Sci Instrum 78:073904

Farber DL, Krisch M, Antonangeli D, Beraud A, Badro J, Occelli F, Orlikowski D (2006) Lattice dynamics of molybdenum at high pressure. Physl Rev Lett 96(11):115502, doi: 10.1103/PhysRevLett.96.115502

Feás X, Fente CA, Hosseini SV, Seijas JA, Vázquez BI, Franco CM, Cepeda A (2009) Use of acrylic acid in the synthesis of molecularly imprinted polymers for the analysis of cyproheptadine. Mater Sci Eng C 29:398-404, doi: 10.1016/j.msec.2008.08.011

Fei Y, Mao HK (1994) In situ determination of the NiAs phase of FeO at high pressure and high temperature. Science 266:1678-1680

Fei YW, Ricolleau A, Frank M, Mibe K, Shen GY, Prakapenka V (2007) Toward an internally consistent pressure scale. Proc Natl Acad Sci 104(22):9182-9186, doi: 10.1073/pnas.0609013104

Fiquet G, Badro J, Guyot F, Requardt H, Krisch M (2001) Sound velocities in iron to 110 gigapascals. Science 291(5503):468-471

Friedrich A, Haussuhl E, Boehler R, Morgenroth W, Juarez-Arellano EA, Winkler B (2007) Single-crystal structure refinement of diaspore at 50 GPa. Am Mineral 92(10):1640-1644, doi: 10.2138/am.2007.2549

Funakoshi K (1995) Energy-dispersive X-ray diffraction study for alkali silicate melts using synchrotron radiation under high pressure and temperature. Ph.D. Dissertation. Tokyo Institute of Technology, 117 p

Galayda JN, Arthur J, Ratner DF, White WE (2010) X-ray free-electron lasers: present and future capabilities. J Opt Soc Am B 27(11):B106-B118

Gasc J, Schubnel A, Brunet F, Guillon S, Mueller H-J, Lathe C (2011) Simultaneous acoustic emissions monitoring and synchrotron X-ray diffraction at high pressure and temperature: Calibration and application to serpentinite dehydration. Phys Earth Planet Inter 189(3–4):121-133, doi: 10.1016/j.pepi.2011.08.003

Goncharov AF (2010) X-ray diffraction in the pulsed laser heated diamond anvil cell. Rev Sci Instrum 81(11):113902

Gorria P, Martínez-Blanco D, Pérez MJ, Blanco JA, Hernando A, Laguna-Marco MA, Haskel D, Souza-Neto N, Smith RI, Marshall WG, Garbarino G, Mezouar M, Fernández-Martínez A, Chaboy J, Fernandez Barquín L, Rodriguez Castrillón JA, Moldovan M, García Alonso JI, Zhang J, Llobet A, Jiang JS (2009) Stress-induced large Curie temperature enhancement in $Fe_{64}Ni_{36}$ Invar alloy. Phys Rev B 80(6): 064421, doi: 10.1103/PhysRevB.80.064421

Gotou H, Yagi T, Frost DJ, Rubie DC (2006) Opposed-anvil-type high-pressure and high-temperature apparatus using sintered diamond. Rev Sci Instrum 77(3):035113-035116

Gotou H, Yagi T, Okada T, Iizuka R, Kikegawa T (2011) A simple opposed-anvil apparatus for high pressure and temperature experiments above 10 GPa. High Pressure Res 31(4):592-602, doi: 10.1080/08957959.2011.618130

Hartman PL (1982) Introductory remarks. Nucl Instrum Methods Phys Res 195(1–2):1-6, doi: http://dx.doi.org/10.1016/0029-554X(82)90749-2

Haskel D, Fabbris G, Souza-Neto NM, Van Veenendaal M, Shen G, Smith AE, Subramanian MA (2011) Stability of the ferromagnetic ground state of La_2MnNiO_6 against large compressive stress. Phys Rev B 84(10):100403

Heinz DL, Jeanloz R (1987) Temperature measurements in the laser heated diamond cell. *In:* High Pressure Researches in Mineral Physics. Manghnani HM, Syono Y (eds) AGU, Washington DC, p 113-127

Hemley RJ, Mao HK, Shen G, Badro J, Gillet P, Hanfland M, Häusermann D (1997) X-ray imaging of stress and strain of diamond, iron, and tungsten at megabar pressures. Science 276:1242

Hemley RJ, Mao HK, Struzhkin VV (2005) Synchrotron radiation and high pressure: new light on materials under extreme conditions. J Synchrotron Radiat 12:135-154

Hilairet N, Reynard B, Wang Y, Daniel I, Merkel S, Nishiyama N, Petitgirard S (2007) High-pressure creep of serpentine, interseismic deformation, and initiation of subduction. Science 318(5858):1910-1913, doi: 10.1126/science.1148494

Hilairet N, Wang Y, Sanehira T, Merkel S, Mei S (2012) Deformation of olivine under mantle conditions: An *in situ* high-pressure, high-temperature study using monochromatic synchrotron radiation. J Geophys Res B 117(1):B01203, doi: 10.1029/2011jb008498

Hirth G, Kohlstedt D (2003) Rheology of the upper mantle and the mantle wedge: A view from the experimentalists. *In:* Inside the Subduction Factory. Eiler J (ed) AGU, Washington DC, p 83-105, doi: 10.1029/138gm06

Hong X, Shen G, Prakapenka VB, Rivers ML, Sutton SR (2007) Density measurements of noncrystalline materials at high pressure with diamond anvil cell. Rev Sci Instrum 78(10):103905

Ice GE, Dera P, Liu WJ, Mao HK (2005) Adapting polychromatic X-ray microdiffraction techniques to high-pressure research: energy scan approach. J Synchrotron Radiat 12:608-617, doi: 10.1107/s0909049505024684

Ice GE, Pang JWL (2009) Tutorial on X-ray microLaue diffraction. Mater Charact 60(11):1191-1201, doi: 10.1016/j.matchar.2009.07.006

Ingalls R, Garcia GA, Stern EA (1978) X-ray absorption at high-pressure. Phys Rev Lett 40(5):334-336, doi: 10.1103/PhysRevLett.40.334

Iota V, Klepeis JHP, Yoo CS, Lang J, Haskel D, Srajer G (2007) Electronic structure and magnetism in compressed 3d transition metals. Appl Phys Lett 90(4):042505, doi: 10.1063/1.2434184

Irifune T, Kurio A, Sakamoto S, Inoue T, Sumiya H (2003) Ultrahard polycrystalline diamond from graphite. Nature 421: 599-600

Ishimatsu N, Matsumoto K, Maruyama H, Kawamura N, Mizumaki M, Sumiya H, Irifune T (2012) Glitch-free X-ray absorption spectrum under high pressure obtained using nano-polycrystalline diamond anvils. J Synchrotron Radiat 19(5):768-772, doi: doi: 10.1107/S0909049512026088

Ito E, Katsura T, Yamazaki D, Yoneda A, Tado M, Ochi T, Nishibara E, Nakamura A (2009) A new 6-axis apparatus to squeeze the Kawai-cell of sintered diamond cubes. Phys Earth Planet Inter 174(1-4):264-269, doi: 10.1016/j.pepi.2008.11.007

Ito E, Yamazaki D, Yoshino T, Fukui H, Zhai S, Shatzkiy A, Katsura T, Tange Y, Funakoshi K-I (2010) Pressure generation and investigation of the post-perovskite transformation in $MgGeO_3$ by squeezing the Kawai-cell equipped with sintered diamond anvils. Earth Planet Science Lett 293(1-2):84-89, doi: 10.1016/j.epsl.2010.02.023

Jackson DD, Aracne-Ruddle C, Malba V, Weir ST, Catledge SA, Vohra YK (2003) Magnetic susceptibility measurements at high pressure using designer diamond anvils. Rev Sci Instrum 74:2467-2471

Jackson JM, Sturhahn W, Lerche M, Zhao J, Toellner TS, Alp EE, Sinogeikin S, Bass JD, Murphy CA, Wicks JK (2013) Melting of compressed iron by monitoring atomic dynamics. Earth Planet Sci Lett 362:143-150

Jackson JM, Sturhahn W, Shen GY, Zhao JY, Hu MY, Errandonea D, Bass JD, Fei YW (2005) A synchrotron Mossbauer spectroscopy study of $(Mg,Fe)SiO_3$ perovskite up to 120 GPa. Am Mineral 90(1): 199-205, doi: 10.2138/am.2005.1633

Jensen BJ, Luo SN, Hooks DE, Fezzaa K, Ramos KJ, Yeager JD, Kwiatkowski K, Shimada T, Dattelbaum DM (2012) Ultrafast, high resolution, phase contrast imaging of impact response with synchrotron radiation. AIP Advances 2(1):012170

Kanzaki M, Kurita K, Fujii T, Kato T, Shimomura O, Akimoto S (1987) A new technique to measure the viscosity and density of silicate melts at high pressure. *In:* High-pressure Research in Mineral Physics. Manghnani MH, Syono Y (eds) Terrapub/AGU, Tokyo, p 195-200

Katayama Y, Mizutani T, Utsumi W, Shimomura O, Yamakata M, Funakoshi K-I (2000) A first order liquid-liquid phase transition in phosphorus. Nature 403:170-173

Katayama Y, Tsuji K, Nosaka H, Yaoita K, Kikegawa T, Shimomura O (1996) Density of liquid tellurium under pressure. J Non-Cryst Solids 205:451-454

Kawazoe T, Nishihara Y, Ohuchi T, Nishiyama N, Higo Y, Funakoshi K-I, Irifune T (2011) In situ stress-strain measurements in a deformation-DIA apparatus at P-T conditions of the upper part of the mantle transition zone. Am Mineral 96(11-12):1665-1672, doi: 10.2138/am.2011.3818

Khvostantsev LG, Vereshchagin LF, Novikov AP (1977) Device of toroid type for high pressure generation. High Temp High Pressure 9:637-639

Komabayashi T, Fei YW (2010) Internally consistent thermodynamic database for iron to the Earth's core conditions. J Geophys Res-Solid Earth 115:B03202, doi: 10.1029/2009jb006442

Kono Y, Irifune T, Higo Y, Inoue T, Barnhoorn A (2009) P-V-T relation of MgO derived by simultaneous elastic wave velocity and *in situ* X-ray measurements: A new pressure scale for the mantle transition region. Phys Earth Planet Inter 183:196-211

Kono Y, Kenney-Benson C, Park C, Shen G, Wang Y (2013) Anomaly in the viscosity of liquid KCl at high pressures. Phys Rev B 87(2):024302

Kubo A, Wang Y, Runge CE, Uchida T, Kiefer B, Nishiyama N, Duffy TS (2008) Melting curve of silicon to 15 GPa determined by two-dimensional angle-dispersive diffraction using a Kawai-type apparatus with X-ray transparent sintered diamond anvils. J Phys Chem Solids 69(9):2255-2260

Kubo T, Ohtani E, Kato T, Urakawa S, Suzuki A, Kanbe Y, Funakoshi K, Utsumi W, Kikegawa T, Fujino K (2002) Mechanisms and kinetics of the post-spinel transformation in Mg_2SiO_4. Phys Earth Planet Inter 129:153-171

Kunimoto T, Irifune T (2010) Pressure generation to 125 GPa using a 6-8-2 type multianvil apparatus with nano-polycrystalline diamond anvils. J Phys Conf Series 215(1):012190

Lavina B, Dera P, Downs RT (2014) Modern X-ray diffraction methods in mineralogy and geosciences. Rev Mineral Geochem 78:1-31

Lavina B, Dera P, Downs RT, Yang WG, Sinogeikin S, Meng Y, Shen GY, Schiferl D (2010) Structure of siderite $FeCO_3$ to 56 GPa and hysteresis of its spin-pairing transition. Phys Rev B 82(6):064110, doi: 10.1103/PhysRevB.82.064110

Le Bolloch D, Itie JP, Polian A, Ravy S (2009) Combining high pressure and coherent diffraction: a first feasibility test. High Pressure Res 29:635-638

Lee KKM, Benedetti LR, Jeanloz R, Celliers PM, Eggert JH, Hicks DG, Moon SJ, Mackinnon A, Da Silva LB, Bradley DK, Unites W, Collins GW, Henry E, Koenig M, Benuzzi-Mounaix A, Pasley J, Neely D (2006) Laser-driven shock experiments on precompressed water: Implications for "icy" giant planets. J Chem Phys 125(1):014701, doi: 10.1063/1.2207618

Lee SK, Eng PJ, Mao HK, Shu JF (2008) Probing and modeling of pressure-induced coordination transformation in borate glasses: Inelastic X-ray scattering study at high pressure. Phys Rev B 78(21):214203, doi: 10.1103/PhysRevB.78.214203

Lesher CE, Wang Y, Gaudio S, Clark A, Nishiyama N, Rivers M (2009) Volumetric properties of magnesium silicate glasses and supercooled liquid at high pressure by X-ray microtomography, Phys Earth Planet Inter 174(1-4):292-301

Li B, Liebermann RC (2007) Indoor seismology by probing the Earth's interior by using sound velocity measurements at high pressures and temperatures. Proc Natl Acad Sciences 104(22):9145-9150, doi: 10.1073/pnas.0608609104

Li L, Weidner DJ (2008) Effect of phase transitions on bulk dispersion and attenuation: implications for the Earth. Nature 454:984-986

Li L, Weidner DJ (2010) Synchronized stress-strain measurements in dynamic loading at high pressure using D-DIA. Rev Sci Instrum 81:473-477

Li B, Kung J, Liebermann RC (2004a) Modern techniques in measuring elasticity of Earth materials at high pressure and high temperature using ultrasonic interferometry in conjunction with synchrotron X-radiation in multi-anvil apparatus. Phys Earth Planet Inter 143-144:559-574

Li J, Struzhkin VV, Mao H-K, Shu J, Hemley RJ, Fei Y, Mysen B, Dera P, Prakapenka V, Shen G (2004b) Electronic spin state of iron in lower mantle perovskite. Proc Natl Acad Sci 101(39):14027-14030, doi: 10.1073/pnas.0405804101

Lin J-F, Fei Y, Sturhahn W, Zhao J, Mao H-K, Hemley RJ (2004) Magnetic transition and sound velocities of Fe3S at high pressure: implications for Earth and planetary cores. Earth Planet Sci Lett 226(1-2):33-40

Lin J-F, Struzhkin VV, Jacobsen SD, Hu MY, Chow P, Kung J, Liu H, Mao H-K, Hemley RJ (2005a) Spin transition of iron in magnesiowüstite in the Earth's lower mantle. Nature 436(7049):377-380

Lin J-F, Sturhahn W, Zhao J, Shen G, Mao HK, Hemley RJ (2005b) Sound velocities of hot dense iron: Birch's law revisited. Science 308:1892-1894

Lin Y, Zhang L, Mao H-K, Chow P, Xiao Y, Baldini M, Shu J, and Mao WL (2011) Amorphous diamond: a high-pressure superhard carbon allotrope. Phys Rev Lett 107(17):175504

Lin J-F, Alp EE, Mao Z, Inoue T, Mccammon C, Xiao Y, Chow P, Zhao J (2012) Electronic spin states of ferric and ferrous iron in the lower-mantle silicate perovskite. Am Mineral 97(4):592-597, doi: 10.2138/am.2012.4000

Loubeyre P, Celliers PM, Hicks DG, Henry E, Dewaele A, Pasley J, Eggert J, Koenig M, Occelli F, Lee KM, Jeanloz R, Neely D, Benuzzi-Mounaix A, Bradley D, Bastea M, Moon S, Collins GW (2004) Coupling static and dynamic compressions: First measurements in dense hydrogen. High Pressure Res 24(1):25-31, doi: 10.1080/08957950310001635792

Loubeyre P, Letoullec R, Hausermann D, Hanfland M, Hemley RJ, Mao HK, Finger LW (1996) X-ray diffraction and equation of state of hydrogen at megabar pressures. Nature 383(6602):702-704

Lübbers R, Grünsteudel HF, Chumakov AI, Wortmann G (2000) Density of phonon states in iron at high pressure. Science 287(5456):1250-1253, doi: 10.1126/science.287.5456.1250

Luo SN, Jensen BJ, Hooks DE, Fezzaa K, Ramos KJ, Yeager JD, Kwiatkowski K, Shimada T (2012) Gas gun shock experiments with single-pulse X-ray phase contrast imaging and diffraction at the Advanced Photon Source. Rev Sci Instrum 83(7):073903

Maddox BR (2006) Pressure-Induced Electronic Phase Transitions in Transition Metal Oxides and Rare Earth Metals. Ph.D. Dissertation. University of California at Davis, Davis, CA, 165 p

Manthilake MaGM, Walte N, Frost DJ (2012) A new multi-anvil press employing six independently acting 8 MN hydraulic rams. High Pressure Res 32(2):195-207, doi: 10.1080/08957959.2012.680450

Mao HK, Xu J, Bell PM (1986) Calibration of the ruby pressure gauge to 800 kbar under quasi-hydrostatic conditions. J Geophys Res 91:4673-4676

Mao HK, Jephcoat AP, Hemley RJ, Finger LW, Zha C-S, Hazen RM, Cox DE (1988) Synchrotron X-ray diffraction measurements of single-crystal hydrogen to 26.5 Gigapascals. Science 239:1131-1134

Mao HK, Wu Y, Chen LC, Shu JF, Jephcoat AP (1990) Static compression of iron to 300 GPa and Fe0.8Ni0.2 alloy to 260 GPa: implications for composition of the core. J Geophys Res 95:21737-21742

Mao HK, Struzhkin VV, Hemley RJ, Kao CC (1997) Synchrotron X-ray spectroscopy at ultrahigh pressures. EOS, Trans Am Geophys Union 78:F774

Mao HK, Shen G, Hemley RJ, Duffy TS (1998a) X-ray diffraction with a double hot plate laser heated diamond cell. *In*: Properties of Earth and Planetary Materials. Manghnani MH, Yagi T (eds) AGU, Washington DC, p 27-34

Mao HK, Shu J, Shen G, Hemley RJ, Li B, Singh AK (1998b) Elasticity and rheology of iron above 200 GPa and the nature of the Earth's inner core. Nature 396:741-743

Mao HK, Xu J, Struzhkin VV, Shu J, Hemley RJ, Sturhahn W, Hu MY, Alp EE, Vocadlo L, Alfè D, Price GD, Gillan MJ, Schwoerer-Böhning M, Häusermann D, Eng P, Shen G, Giefers H, Lübbers R, Wortmann D (2001) Phonon density of states of iron up to 153 Gigapascals. Science 292:914-916

Mao WL, Mao HK, Eng PJ, Trainor TP, Newville M, Kao CC, Heinz DJ, Shu JF, Meng Y, Hemley RJ (2003) Bonding changes in compressed superhard graphite. Science 302:425-427

Mao HK, Shirley EL, Ding Y, Eng P, Cai YQ, Chow P, Xiao Y, Shu J, Hemley RJ, Kao C, Mao WL (2010) Electronic structure of crystalline ^{4}He at high pressures. Phys Rev Lett 105(18):186404, doi: 10.1103/PhysRevLett.105.186404

Mayanovic RA, Anderson AJ, Bassett WA, Chou IM (2007a) Synchrotron X-ray spectroscopy of Eu/HNO_3 aqueous solutions at high temperatures and pressures and Nb-bearing silicate melt phases coexisting with hydrothermal fluids using a modified hydrothermal diamond anvil cell and rail assembly. Rev Sci Instrum 78(5) doi:10.1063/1.2737748

Mayanovic RA, Anderson AJ, Bassett WA, Chou IM (2007b) Synchrotron X-ray spectroscopy of Eu/HNO_3 aqueous solutions at high temperatures and pressures and Nb-bearing silicate melt phases coexisting with hydrothermal fluids using a modified hydrothermal diamond anvil cell and rail assembly. Rev Sci Instrum 78(5):053904

Mckelvy MJ, Chizmeshya AVG, Diefenbacher J, Béarat H, Wolf G (2004) Exploration of the role of heat activation in enhancing serpentine carbon sequestration reactions. Environ Sci Technol 38:6897-6903

Mei Q, Sinogeikin S, Shen G, Amin S, Benmore CJ, Ding K (2010) High-pressure X-ray diffraction measurements on vitreous GeO_2 under hydrostatic conditions. Phys Rev B 81(17):174113, doi: 10.1103/PhysRevB.81.174113

Meng Y, Weidner DJ, Fei Y (1993) Deviatoric stress in a quasi-hydrostatic diamond anvil cell: effect on the volume based pressure calibration. Geophys Res Lett 20:1147-1149

Merkel S, Kubo A, Miyagi L, Speziale S, Duffy TS, Mao H-K, Wenk H-R (2006) Plastic deformation of $MgGeO_3$ post-perovskite at lower mantle pressures. Science 311(5761):644-646, doi: 10.1126/science.1121808

Mezouar M (2002) Multichannel collimator for structural investigation of liquids and amorphous materials at high pressures and temperatures. Rev Sci Instrum 73(10):3570

Mezouar M (2010) Synchrotron high-pressure high-temperature techniques. *In:* High-Pressure Crystallography. Boldyreva E, Dera P (eds) Springer Netherlands, p 23-33, doi: 10.1007/978-90-481-9258-8_3

Mezouar M, Faure P, Crichton W, Rambert N, Sitaud B, Bauchau S, Blattmann G (2002) Multichannel collimator for structural investigation of liquids and amorphous materials at high pressures and temperatures. Rev Sci Instrum 73:3570-3574

Mills DM (2002) Third-Generation Hard X-ray Synchotron Radiation Sources. John Wiley & Sons, Inc., New York

Ming LC, Bassett WA (1974) Laser heating in the diamond anvil press up to 2000 °C sustained and 3000 °C pulsed at pressures up to 260 kilobars. Rev Sci Instrum 9:1115-1118

Miyagi L, Kanitpanyacharoen W, Kaercher P, Lee KKM, Wenk HR (2010) Slip systems in $MgSiO_3$ post-perovskite: implications for D'' anisotropy. Science 329(5999):1639-1641, doi: 10.1126/science.1192465

Morard G (2011) High efficiency multichannel collimator for structural studies of liquids and low-Z materials at high pressures and temperatures. Rev Sci Instrum 82(2):023904

Morard G, Mezouar M, Rey N, Poloni R, Merlen A, Le Floch S, Toulemonde P, Pascarelli S, San-Miguel A, Sanloup C, Fiquet G (2007a) Optimization of Paris–Edinburgh press cell assemblies for *in situ* monochromatic X-ray diffraction and X-ray absorption. High Pressure Res 27(2):223-233

Morard G, Sanloup C, Fiquet G, Mezouar M, Rey N, Poloni R, Beck P (2007b) Structure of eutectic Fe-FeS melts to pressures up to 17 GPa: Implications for planetary cores. Earth Planet Sci Lett 263(1-2):128-139

Morard G, Sanloup C, Guillot B, Fiquet G, Mezouar M, Perrillat JP, Garbarino G, Mibe K, Komabayashi T, Funakoshi K (2008) In situ structural investigation of Fe-S-Si immiscible liquid system and evolution of Fe-S bond properties with pressure. J Geophys Res 113, doi: 10.1029/2008jb005663

Murphy CA, Jackson JM, Sturhahn W, Chen B (2011a) Grüneisen parameter of hcp-Fe to 171 GPa. Geophys Res Lett 38(24):L24306, doi: 10.1029/2011gl049531

Murphy CA, Jackson JM, Sturhahn W, Chen B (2011b) Melting and thermal pressure of hcp-Fe from the phonon density of states. Phys Earth Planet Inter 188(1–2):114-120, doi: 10.1016/j.pepi.2011.07.001

Nasu S (1996) High pressure Mossbauer spectroscopy with nuclear forward scattering of synchrotron radiation. High Pressure Res 14:405-412

Nishiyama N, Wang Y, Irifune T, Sanehira T, Rivers ML, Sutton SR, Cookson D (2009) A combination of a Drickamer anvil apparatus and monochromatic X-rays for stress and strain measurements under high pressure. J Synchrotron Radiat 16(6):742-747, doi: 10.1107/S0909049509033342

Nishiyama N, Wang Y, Rivers ML, Sutton SR, Cookson D (2007) Rheology of ε-iron up to 19 GPa and 600 K in the D-DIA. Geophys Res Lett 34, doi: 10.1029/2007gl031431

Ohtani E (1979) Melting relation of Fe_2SiO_4 up to about 200 kbar. J Phys Earth 27:189-208

Ohtani E, Kagawa N, Shimomura O, Togaya M, Suito K, Onodera A, Sawamoto H, Yoneda M, Tanaka S, Utsumi W, Ito E, Matsumuro A, Kikegawa T (1989) High pressure generation by a multiple anvil system with sintered diamond anvils. Rev Sci Instrum 60:922-925

Ohuchi T, Kawazoe T, Nishiyama N, Nishihara Y, Irifune T (2010) Technical development of simple shear deformation experiments using a deformation-DIA aparatus. J Earth Sci 21:523-531, doi: 10.1007/s12583-010-0110-4

Osugi J, Shimizu K, Inoue K, Yasunami K (1964) A compact cubic anvil high pressure apparatus. Rev Phys Chem Jpn 34:1-6

Pacold JI, Bradley JA, Mattern BA, Lipp MJ, Seidler GT, Chow P, Xiao X, Rusthoven B, Quintana J (2012) A miniature X-ray emission spectrometer (miniXES) for high pressure studies in a diamond anvil cell. J Synchroton Radiat 19:245-251

Pascarelli S, Mathon O (2010) Advances in high brilliance energy dispersive X-ray absorption spectroscopy. Phys Chem Chem Phys 12(21):5535-5546, doi: 10.1039/b926509k

Petitgirard S, Daniel I, Dabin Y, Cardon H, Tucoulou R, Susini J (2009) A diamond anvil cell for X-ray fluorescence measurements of trace elements in fluids at high pressure and high temperature. Rev Sci Instrum 80(3):033906

Pfeifer MA, Williams GJ, Vartanyants IA, Harder R, Robinson IK (2006) Three-dimensional mapping of a deformation field inside a nanocrystal. Nature 442(7098):63-66

Pinceaux J-P, Maury J-P, Besson J-M (1979) Solidification of helium, at room temperature under high pressure. J Phys Lett 40(13):307-308

Ping Y, Landen OL, Hicks DG, Koch JA, Wallace R, Sorce C, Hammel BA, Collins GW (2011) Refraction-enhanced X-ray radiography for density profile measurements at CH/Be interface. J Instrum 6:P09004, doi: 10.1088/1748-0221/6/09/p09004

Rietveld HM (1966) A method for including line profiles of neutron powder diffraction peaks in determination of crystal structures. Acta Crystallogr S 21:A228

Rueff J-P (2010) An introduction to inelastic X-ray scattering. *In:* Magnetism and Synchrotron Radiation. Springer Proceedings in Physics, Volume 133. Beaurepaire E, Bulou H, Scheurer F, Jean-Paul K (eds) Springer-Verlag, Berlin, Heidelberg, p 263-277

Rueff J-P, Kao CC, Struzhkin VV, Badro J, Shu J, Hemley RJ, Mao HK (1999) Pressure-induced high-spin to low-spin transition in FeS evidenced by X-ray emission spectroscopy. Phys Rev Lett 82:3284-3287

Rutter MD, Secco RA, Uchida T, Liu HJ, Rivers ML, Sutton SR, Wang Y (2002) Viscosity of liquid Fe at high pressure. Phys Rev B 66:060102

Sakamaki T, Wang Y, Park C, Yu T, Shen G (2012) Structure of jadeite melt at high pressures up to 4.9 GPa. J Appl Phys 111(11):112623

Schell N, Simmons RO, Kaprolat A, Schulke W, Burkel E (1995) Electronic excitations in hcp He at 61.5 MPa and 4.3 K studied by inelastic X-ray-scattering spectroscopy. Phys Rev Lett 74(13):2535-2538, doi: 10.1103/PhysRevLett.74.2535

Schmidt C, Rickers K (2003) In-situ determination of mineral solubilities in fluids using a hydrothermal diamond-anvil cell and SR-XRF: Solubility of AgCl in water. Am Mineral 88(2-3):288-292

Schmidt C, Rickers K, Bilderback DH, Huang R (2007) In situ synchrotron-radiation XRF study of REE phosphate dissolution in aqueous fluids to 800 degrees C. Lithos 95(1-2):87-102, doi: 10.1016/j.lithos.2006.07.017

Schubnel A, Brunet F, Hilairet N, Gasc J, Wang Y, Green Ii HW (2013) Deep focus earthquake analogs recorded at high pressure and temperature in the laboratory. Science 341:1377-1380, doi: 10.1126/science.1240206

Seal M (1963) The effect of surface orientation on the graphitization of diamond. Phys Status Solidi B 3(4):658-664, doi: 10.1002/pssb.19630030408

Shen G, Mao HK, Hemley RJ (1996) Laser-heating diamnd-anvil cell technique: Double-sided heating with multimode Nd:YAG laser. Presented at Advanced Materials '96 - New Trends in High Pressure Research, NIRIM, NIRIM, Tsukuba, Japan. *http://www.hpcat.aps.anl.gov/shen/publication/shen-Japan96.pdf* (accessed August 1, 2013)

Shen G, Rivers ML, Wang Y, Sutton SJ (2001) A laser heated diamond cell system at the Advanced Photon Source for *in situ* X-ray measurements at high pressure and temperature. Rev Sci Instrum 72:1273-1282

Shen G, Sata N, Newville M, Rivers ML, Sutton SR (2002) Molar volumes of molten indium at high pressures measured in a diamond anvil cell. Appl Phys Lett 81(8):1411-1413

Shen G, Prakapenka VB, Rivers ML, Sutton SR (2003) Structural investigation of amorphous materials at high pressures using the diamond anvil cell. Rev Sci Instrum 74:3021-3026

Shen G, Chowa P, Xiaoa Y, Sinogeikina S, Menga Y, Yanga W, Liermanna H-P, Shebanovaa O, Roda E, Bommannavara A, Maoa H-K (2008) HPCAT: an integrated high-pressure synchrotron facility at the Advanced Photon Source. High Pressure Res 28:145-162

Shen G, Wang L, Ferry R, Mao HK, Hemley RJ (2010) A portable laser heating microscope for high pressure research. J Phys 215:012191

Shim S-H, Bengtson A, Morgan D, Sturhahn W, Catalli K, Zhao J, Lerche M, Prakapenka V (2009) Electronic and magnetic structures of the postperovskite-type Fe_2O_3 and implications for planetary magnetic records and deep interiors. Proc Natl Acad Sci 106(14):5508-5512, doi: 10.1073/pnas.0808549106

Shimomura O, Utsumi W, Taniguchi T, Kikegawa T, Nagashima T (1992) A new high pressure and high temperature apparatus with sintered diamond anvils for synchrotron radiation use. *In:* High-Pressure Research: Application to Earth and Planetary Sciences. Syono Y, Manghnani MH (eds) Terra Scientific Co., Tokyo, p 3-11

Shukla A, Rueff JP, Badro J, Vanko G, Mattila A, De Groot FMF, Sette F (2003) Charge transfer at very high pressure in NiO. Phys Rev B 67(8), doi: 10.1103/PhysRevB.67.081101

Sinogeikin S, Bass J, Prakapenka V, Lakshtanov D, Shen GY, Sanchez-Valle C, Rivers M (2006) Brillouin spectrometer interfaced with synchrotron radiation for simultaneous X-ray density and acoustic velocity measurements. Rev Sci Instrum 77(10):103905, doi: 10.1063/1.2360884

Skelton EF, Kirkland J, Qadri SB (1982) Energy-dispersive measurements of diffracted synchrotron radiation as a function of pressure: applications to phase transitions in KCl and KI. J Appl Crystallogr 15(1):82-88, doi: 10.1107/S002188988201139X

Smith RF, Pollaine SM, Moon SJ, Lorenz KT, Celliers PM, Eggert JH, Park HS, Collins GW (2007) High planarity X-ray drive for ultrafast shockless-compression experiments. Phys Plasmas 14(5):057105, doi: 10.1063/1.2712450

Soignard E, Benmore CJ, Yarger JL (2010) A perforated diamond anvil cell for high-energy X-ray diffraction of liquids and amorphous solids at high pressure. Rev Sci Instrum 81(3):035110, doi: 10.1063/1.3356977

Souza-Neto NM, Zhao J, Alp EE, Shen G, Sinogeikin SV, Lapertot G, Haskel D (2012) Reentrant valence transition in EuO at high pressures: beyond the bond-valence model. Phys Rev Lett 109(2):026403

Speziale S, Milner A, Lee VE, Clark SM, Pasternak MP, Jeanloz R (2005) Iron spin transition in Earth's mantle. Proc Natl Acad Sci USA 102(50):17918-17922, doi: 10.1073/pnas.0508919102

Struzhkin VV, Mao HK, Lin J-F, Hemley RJ, Tse JS, Ma Y, Hu MY, Chow P, Kao C-C (2006) Valence band X-ray emission spectra of compressed germanium. Phys Rev Lett 96:137402

Sturhahn W (2004) Nuclear resonant scattering. J Phys Condens Matter 16:S497-S530

Suggit M, Kimminau G, Hawreliak J, Remington B, Park N, Wark J (2010) Nanosecond X-ray Laue diffraction apparatus suitable for laser shock compression experiments. Rev Sci Instrum 81(8):083902, doi: 10.1063/1.3455211

Takemura K (2001) Evaluation of the hydrostaticity of a helium pressure medium with powder X-ray diffraction techniques. J Appl Phys 89:662-668

Tange Y, Irifune T, Funakoshi K-I (2008) Pressure generation to 80 GPa using multianvil apparatus with sintered diamond anvils. High Pressure Res 28(3):245-254

Tanis EA, Simon A, Tschauner O, Chow P, Xiao Y, Shen G, Hanchar JM, Frank M (2012) Solubility of xenotime in a 2 M HCl aqueous fluid from 1.2 to 2.6 GPa and 300 to 500 °C. Am Mineral 97(10):1708-1713, doi: 10.2138/am.2012.4009

Terasaki H, Urakawa S, Funakoshi K-I, Wang Y, Shibazaki Y, Sanehira T, Ueda Y, Ohtani E (2008) Interfacial tension measurement of Ni-S liquid using high-pressure X-ray micro-tomography. High Pressure Res 28(3):327-334

Tsuji K, Yaoita K, Imai M, Shimomura O, Kikegawa T (1989) Measurements of X-ray diffraction for liquid metals under high pressure. Rev Sci Instrum 60(7):2425-2428

Turneaure SJ, Gupta YM, Zimmerman K, Perkins K, Yoo CS, Shen G (2009) Real-time microstructure of shocked LiF crystals: Use of synchrotron X-rays. J Appl Phys 105(5):053520

Uchida T, Wang Y, Nishiyama N, Funakoshi K-I, Kaneko H, Nozawa A, Von Dreele RB, Rivers ML, Sutton SR, Yamada A, Kunimoto T, Irifune T, Inoue T, Li B (2009) Non-cubic crystal symmetry of $CaSiO_3$ perovskite up to 18 GPa and 1600 K. Earth Planet Sci Lett 282(1-4):268-274

Uhoya W, Tsoi G, Vohra Y, Wolanyk N, Rao SM, Wu M-K, Weir S (2012) Simultaneous measurement of pressure evolution of crystal structure and superconductivity in FeSe 0.92 using designer diamonds. Europhys Lett 99(2):26002

Urakawa S, Terasaki H, Funakoshi K, Uesugi K, Yamamoto S (2010) Development of high pressure apparatus for X-ray microtomography at SPring-8. J Phys Conf Ser 215(1):012026

Utsumi W, Funakoshi K, Urakawa S, Yamakata M, Tsuji K, Konishi H, Shimomura O (1998) SPring-8 beamlines for high pressure science with multi-anvil apparatus. Rev High Pressure Sci Technol 7:1484-1490

Vaughan MT (1993) In situ X-ray diffraction using synchrotron radiation at high P and T in a multi-anvil device. *In:* Experiments at High Pressure and Applications to the Earth's Mantle, Short Course Handbook. Luth RW (ed) Mineralogical Association of Canada, Edmonton, Canada, p 95-130

Wang Y (2010) Large volume presses for high-pressure studies using synchrotron radiation. *In:* High-Pressure Crystallography. Boldyreva E, Dera P (eds) Springer Netherlands, p 81-96, doi: 10.1007/978-90-481-9258-8_8

Wang Y, Shen G, Rivers M, Sutton S (1998) A multi-anvil high pressure system with synchrotron X-ray probe: New opportunities for in-situ materials research at simultaneously high pressure and temperature. MRS Proceedings 499, http://dx.doi.org/10.1557/PROC-499-289

Wang Y, Rivers M, Uchida T, Murray P, Shen G, Sutton S, Chen J, Xu Y, Weidner D (2000) High pressure research using large-volume presses at GeoSoilEnviroCARS, Advanced Photon Source. AIRAPT-17:1047-1052

Wang Y, Shen G, Rivers M (2002a) High pressure research in third generation synchrotron sources. *In:* Third Generation Synchrotron Sources. Mills D (ed) Wiley and Son, New York, p 203-235

Wang Y, Shen G, Rivers ML (2002b) High pressure research techniques at third generation synchrotron radiation sources. *In:* Third-generation Hard X-ray Synchrotron Radiation Sources. Mills DM (ed) John Wiley & Sons, New York, p 203-236

Wang Y, Durham WB, Getting IC, Weidner DJ (2003) The deformation-DIA: A new apparatus for high temperature triaxial deformation to pressures up to 15 GPa. Rev Sci Instrum 74:3002-3011

Wang Y, Uchida T, Von Dreele RB, Rivers ML, Nishiyama N, Funakoshi K, Nozawa A, Kaneko H (2004) A new technique for angle-dispersive powder diffraction using an energy-dispersive setup and synchrotron radiation. J Appl Crystallogr 37(6):947-956, doi: 10.1107/S0021889804022502

Wang Y, Uchida T, Westferro F, Rivers ML, Nishiyama N, Gebhardt J, Lesher CE, Sutton SR (2005a) High-pressure X-ray tomography microscope: Synchrotron computed microtomography at high pressure and temperature. Rev Sci Instrum 76(7):073709

Wang Y, Uchida T, Westferro F, Rivers ML, Nishiyama N, Gebhardt J, Lesher CE, Sutton SR (2005b) High-pressure x-ray tomography microscope: synchrotron computed microtomography at high pressure and temperature. Rev Sci Instrum 40(21):5763-5766, doi: 10.1007/s10853-005-2476-8

Wang Y, Rivers M, Sutton S, Nishiyama N, Uchida T, Sanehira T (2009) The large-volume high-pressure facility at GSECARS: A "Swiss-army-knife" approach to synchrotron-based experimental studies. Phys Earth Planet Inter 174(1-4): 270-281

Wang S, Mao WL, Sorini AP, Chen C-C, Devereaux TP, Ding Y, Xiao Y, Chow P, Hiraoka N, Ishii H, Cai YQ, Kao C-C (2010a) High-pressure evolution of Fe_2O_3 electronic structure revealed by X-ray absorption. Phys Rev B 82(14):144428

Wang Y, Jing Z, Hilairet N, Yu T, Nishiyama N, Tange Y, Sakammaki T, Rivers M, Sutton S (2010b) DDIA-30: a versatile megabar mutlianvil device for in-situ high pressure studies with white and monochromatic synchrotron radiation. Eos Trans AGU: MR13A-1908

Wang Y, Lesher C, Fiquet G, Rivers ML, Nishiyama N, Siebert J, Roberts J, Morard G, Gaudio S, Clark A, Watson H, Menguy N, Guyot F (2011) In situ high-pressure and high-temperature X-ray microtomographic imaging during large deformation: A new technique for studying mechanical behavior of multiphase composites. Geosphere 7(1):40-53, doi: 10.1130/ges00560.1

Wang J, Yang W, Wang S, Xiao X, De Carlo F, Liu Y, Mao WL (2012) High pressure nano-tomography using an iterative method. J Appl Phys 111(11):112626-112625

Wenk HR, Ischia G, Nishiyama N, Wang Y, Uchida T (2005) Texture development and deformation mechanisms in ringwoodite. Phys Earth Planet Inter 152(3):191-199

Wenk HR, Lonardelli I, Pehl J, Devine J, Prakapenka V, Shen G, Mao HK (2004) In situ observation of texture development in olivine, ringwoodite, magnesiowustite and silicate perovskite at high pressure. Earth Planet Sci Lett 226(3-4):507-519, doi: 10.1016/j.epsl.2004.07.033

Wenk HR, Matthies S, Hemley RJ, Mao HK, Shu JF (2000) The plastic deformation of iron at pressures of the Earth's inner core. Nature 405:1044-1047

Wicks JK, Jackson JM, Sturhahn W (2010) Very low sound velocities in iron-rich (Mg,Fe)O: Implications for the core-mantle boundary region. Geophys Res Lett 37(15):L15304, doi: 10.1029/2010gl043689

Wilding MC, Wilson M, Mcmillan PF (2006) Structural studies and polymorphism in amorphous solids and liquids at high pressure. Chem Soc Rev 35(10):964-986

Wilke M, Appel K, Vincze L, Schmidt C, Borchert M, Pascarelli S (2010) A confocal set-up for micro-XRF and XAFS experiments using diamond-anvil cells. J Synchrotron Radiat 17:669-675, doi: 10.1107/s0909049510023654

Yamada A, Wang YB, Inoue T, Yang WG, Park C, Yu T, Shen GY (2011) High-pressure X-ray diffraction studies on the structure of liquid silicate using a Paris-Edinburgh type large volume press. Rev Sci Instrum 82(1):015103, doi: 10.1063/1.3514087

Yamanaka T, Ogata K (1991) Structure refinement of GeO_2 polymorphs at high pressures and temperatures by energy-dispersive spectra of powder diffraction. J Appl Crystallogr 24:111-118

Yamazaki D, Karato S (2001) High pressure rotational deformation apparatus to 15 GPa. Rev Sci Instrum 72:4207-4211

Yang W, Huang X, Harder R, Clark JN, Robinson IK, Mao H-K (2013) Coherent diffraction imaging of nanoscale strain evolution in a single crystal under high pressure. Nat Commun 4:1680, doi: 10.1038/ncomms2661

Yaoita K (1997) Angle-dispersive diffraction measurement system for high-pressure experiments using a multichannel collimator. Rev Sci Instrum 68(5):2106-2110

Yoo CS, Wei H, Chen JY, Shen G, Chow P, Xiao X (2011) Time- and angle-resolved X-ray diffraction to probe structural and chemical evolution during Al-Ni intermetallic reactions. Rev Sci Instrum 82:113901-113906

Yoshiasa A, Nagai T, Ohtaka O, Kamishima O, Shimomura O (1999) Pressure and temperature dependence of EXAFS Debye-Waller factors in diamond-type and white-tin-type germanium. J Synchrotron Radiat 6(1):43-49, doi: doi: 10.1107/S0909049598011947

Zeng Q, Ding Y, Mao WL, Yang W, Sinogeikin SV, Shu J, Mao H-K, Jiang JZ (2010) Origin of pressure-induced polyamorphism in $Ce_{75}Al_{25}$ metallic glass. Phys Rev Lett 104(10):105702

Zeng Q, Sheng HW, Ding Y, Wang L, Yang W, Jiang JZ, Mao WL, Mao H-K (2011) Long-range topological order in metallic glass. Science 332(6036):1404-1406, doi: 10.1126/science.1200324

Zha CS, Bassett WA (2003) Internal resistive heating in diamond anvil cell for *in situ* X-ray diffraction and Raman scattering. Rev Sci Instrum 74:1225-1262

Zhang L, Meng Y, Dera P, Yang W, Mao WL, Mao H-K (2013) Single-crystal structure determination of (Mg,Fe) SiO_3 postperovskite. Proc Natl Acad Sci 110(16):6292-6295, doi: 10.1073/pnas.1304402110

Zhao J, Sturhahn W, Lin JF, Shen G, Alp EE, Mao HK (2004) Nuclear resonant scattering at high pressure and high temperature. High Pressure Res 24:447-457

Zhao YC, Barvosa-Carter W, Theiss SD, Mitha S, Aziz MJ, Schiferl D (1998) Pressure measurement at high temperature using ten Sm : YAG fluorescence peaks. J Appl Phys 84(8):4049-4059, doi: 10.1063/1.368693